CENTRO DE INVESTIGACIÓN Y ESTUDIOS AVANZADOS DEL INSTITUTO POLITÉCNICO NACIONAL

UNIDAD ZACATENCO

DEPARTAMENTO DE BIOMEDICINA MOLECULAR

“Participación de cortactina en la transmigración de la línea celular murina 6645/4 de leucemia linfoblástica aguda tipo T”

TESIS

Que presenta

QFB. Ramón Castellanos Martínez

Para obtener el grado de

MAESTRO EN CIENCIAS

EN LA ESPECIALIDAD DE

BIOMEDICINA MOLECULAR

Director de Tesis:

Dr. Michael Schnoor

Ciudad de México **Agosto 2018**

CENTER FOR RESEARCH AND ADVANCED STUDIES OF THE NATIONAL POLYTECHNIC INSTITUTE (CINVESTAV)

ZACATENCO UNIT

DEPARTAMENT OF MOLECULAR BIOMEDICINE

"Participation of cortactin in the transmigration of the murine T cell acute lymphoblastic leukemia cell line 6645/4"

THESIS

Presented by

QFB. Ramón Castellanos Martínez

To obtain the degree of

MASTER IN SCIENCES

IN THE SPECIALTY OF

MOLECULAR BIOMEDICINE

Thesis Director:

Dr. Michael Schnoor

Mexico City **August 2018**

ACKNOWLEDGEMENTS

To National Council for Science and Technology (CONACYT), for the scholarship during the period comprised 2016-2018.

To Dr. Michael Schnoor for accepting me as part of their team and for being my mentor in researching.

To my committee Dra. Rosana Pelayo, Dr. Leopoldo Santos and Dr. Vianey Ortíz, for all your good observations and recomendations.

To the MVZ Ricardo Gaxiola Centeno and MVZ Benjamin Emmanuel Chávez Álvarez, and technicians Victor Manuel García Gómez and Felipe Cruz Martínez for their assistance in animal care and handling.

To my dear partners from Schnoor Lab, MSc (to be) Idaira Guerrero, MSc Sandra Chánez, PhD Martha Velázquez, MSc Karla Castro, PhD Hilda Vargas, PhD Eduardo Vadillo, PhD Alexander, for your friendship and support.

To my beloved friends David Cisneros, Perla Salvio, and all from Baja California, for your good vibes and wishes, even in the distance.

To my partner in crime, Gabriela Osuna, for always cheering me up. Thank for everything!!.

DEDICATORY

To my parents, Ramón Castellanos and Olivia Martínez, and to my family... needless to say.

Content

ABBREVIATIONS

°C	Centigrade grades
µg	Micrograms
µL	Microliters
µm	Micrometers
µM	Micromolar
3D	3-dimensional
ABP	Actin-binding protein
AML	Acute myeloid leukemia
APC	Allophycocyanin
ATL	Adult T-cell leukemia/lymphoma
B-CLL	B-cell chronic lymphocytic leukemia
BM	Bone marrow
BSA	Bovine serum albumin
CD#	Cluster differentiation #
cDNA	Complementary DNA
CML	Chronic myeloid leukemia
CNS	Central nervous system
CSC	Cancer stem cell
CTTN	Cortactin
DEPC	Diethyl pyrocarbonate
DMEM	Dulbecco modified Eagle’s Medium
DMSO	Dimethyl sulfoxide
DNA	Deoxyribonucleic acid

dNTPs	Deoxynucleotid triphosphate
DTT	Ditiotreithol
EC	Endothelial cells
ECGF	Endothelial cell growth factor
EDTA	Ethylendiaminetetraacetic acid
ETP-ALL	Early T-cell precursor acute lymphoblastic leukemia
FBS	Fetal bovine serum
GAPDH	Glyceraldehyde-P-dehidrogenase
GSI	γ-secretase inhibitors
HBSS	Hank's balanced saline solution
HEPES	N-(2-Hydroxyethyl)piperazine-N′-(2-ethanesulfonic acid)
HEV	High endothelial venules
HRP	Horse raddish peroxidase
HS1	Hematopoietic cell-specific 1
HSC	Hematopoietic stem cells
HTLV-1	Human T-cell lymphotrophic virus-1
HUVEC	Human umbilical venule endothelial cells
ICAM-1	Intercellular adhesion molecule-1
IL-#	Interleukin #
IMDM	Iscove's modified Dulbecco's Medium
JAM	Junctional adhesion molecule
KDa	Kilodaltons
LFA-1	Leucocyte function-associated antigen-1
LIC	Leukemia-initiating cell
LN	Lymph node

LPS	Lipopolysaccharide
M	Molar
MadCAM-1	Mucosal addresin cell adhesion molecule-1
mg	Milligrams
min	Minutes
mL	Milliliters
MLEC	Murine lung endothelial cells
mm	Millimeters
mM	Millimolar
MMP-9	Matrix metalloproteinase-9
Na_3VO_4	Sodium orthovanadate
NaF	Sodium fluoride
NEAA	Non-essential aminoacids
ng	Nanograms
NIH	National Institute of Health
nM	Nanomolar
NPF	Nucleation promoter factor
NSG	NOD-*scid* IL2Rgamma^{null}
NTA	N-terminal acidic
NTC	Non-tumorigenic cells
OPN	Osteopontin
PBS	Phosphate buffered saline
PCR	Polymerase chain reaction
PE	Phycoerythrin
PECAM-1	Platelet/Endothelial cell adhesion molecule-1

PNAd	Peripheral node addressins
PSGL-1	P-selectin glycoprotein ligand-1
Pyk-2	Proline-rich tyrosine kinase-2
RNA	Ribonucleic acid
rpm	Revolutions per minute
RT	Room temperature
s	Seconds
SDF-1α	Stromal-derived factor-1α
SDS	Sodium dodecyl sulfate
SH3	Scr homology 3
SV#	Splicing variant #
T-ALL	T-cell acute lymphoblastic leukemia
TBS	Tris buffer saline
TC	Tumorigenic cells
TCR	T-cell receptor
TEM	Transendothelial migration
TEMED	N,N,N',N-Tetramethylethylenediamine
TLR	Toll-like receptor
TNF-α	Tumor necrosis factor-α
U	Units
USA	United States of America
V	Volts
VCAM-1	Vascular cell adhesion molecule-1
VLA-4	Very late antigen -1
WT	Wild-type

LIST OF FIGURES

LIST OF TABLES

1. Resumen

La leucemia linfoblástica aguda de células T (LLA-T) se considera como una neoplasia agresiva debido a sus altas tasas de infiltración a médula ósea, sistema nervioso central y testículos. Las recaídas son frecuentes en LLA-T, el cual es el principal obstáculo en la cura de esta enfermedad. Dentro de los casos de leucemias, 25% y 15% corresponden a leucemia linfoblástica aguda de células T en adultos y niños, respectivamente. La extravasación es necesaria para la infiltración de células de LLA-T, proceso migratorio que depende principalmente de la dinámica del citoesqueleto de actina. Cortactina es una que regula el remodelamiento de actina, y por lo tanto la migración celular. Altos niveles de cortactina han sido asociados con la invasividad de varios tipos de cánceres sólidos. Además, en la leucemia linfocítica crónica de células B en adultos, la expresión de cortactina se ha correlacionado con un pronóstico desfavorable.

En el presente trabajo caracterizamos a la línea celular murina 6645/4 de LLA-T, e investigamos si el gran potencial infiltrativo de esta leucemia se correlaciona con altos niveles de expresión de cortactina. Encontramos que la línea celular 6645/4 expresa el marcador CD3 de células T. Por otro lado, la expresión de CD8 fue baja mientras que CD4 estaba ausente. Además, encontramos que estas células se encuentran arrestadas en el estadio doble negativo 3 de maduración de células T, lo que podría indicar un fenotipo similar al de la LLA de precursores tempranos de células T. De manera importante, comparado con células T normales, la línea celular 6645/4 expresaba niveles altos de cortactina, la integrina VLA-4 y CXCR4, proteínas requeridas para la migración. De manera importante, la expresión de cortactina, así como CXCR4 se encontraba varias veces incrementadas en comparación con las células T normales. Cabe resaltar que la expresión de HS1, proteína homóloga a cortactina que también se ha encontrado incrementada en la B-CLL y la preB-ALL, fue muy similar entre las células T leucémicas y normales. Los ensayos de migración transendotelial demostraron que tanto las células T normales como las leucémicas poseen una expresión de cortactina al transmigrar en respuesta a CXCL12, aunque el número de células leucémicas que transmigró fue mayor. Estos resultados sugieren que cortactina juega un papel importante en la infiltración de LLA-T y posiblemente contribuya al entendimiento de la agresividad de esta enfermedad. Además, nuestros resultados sugieren a cortactina como un potencial blanco farmacológico.

1. Abstract

T-cell acute lymphoblastic leukemia (T-ALL) is an aggressive neoplasm due to its high rates of infiltration to bone marrow, central nervous system and testicles. T-ALL relapses frequently, which is a major obstacle for curing the disease. T-ALL accounts for 25% of leukemia cases in adults and 15% in children. Infiltration of T-ALL cells requires extravasation, a migratory process highly dependent on actin cytoskeleton dynamics. Cortactin is an actin-binding protein that regulates actin remodeling and thus cell migration. High expression of cortactin is associated with invasiveness in several types of solid tumors. Moreover, expression of cortactin in adult B-cell chronic lymphocytic leukemia was correlated with negative prognostic factors.

In this work, we characterized the murine T-cell acute lymphoblastic leukemia cell line 6645/4, and investigated whether high levels of cortactin correlate with the infiltrative potential of this disease. We found that 6645/4 cells expressed the CD3 T cell marker. While CD8 levels were low and CD4 was absent. In addition, this cell line shows to be in double negative 3. Of note, compared to normal T cells, 6645/4 cells expressed significantly higher levels of cortactin, the integrin VLA-4 and CXCR4, molecules required for T cell extravasation. Of note, HS1, the cortactin homologue, which is highly overexpressed in both B-CLL and preB-ALL, was similarly expressed in 6645/4 cells when compared to normal T cells. Transendothelial migration assays showed that both 6645/4 leukemic T cells and normal T cells have high levels of cortactin after transmigrating towards a CXCL12 gradient. Importantly, the number of transmigrated 6645/4 cells was significantly higher. Taken together, these results highlight an important role of cortactin in T-ALL infiltration and might contribute to understanding the aggressiveness of this disease. Moreover, these findings suggest cortactin to be a potential pharmacological target to prevent T-ALL infiltration.

2. Introduction

2.1 T-cell Acute Lymphoblastic Leukemia (T-ALL)

2.1.1 T-ALL epidemiology

According to the World Health Organization (WHO) in 2012, leukemia occupied the 11th place in the worldwide cancer statistics, just behind non-Hodgkin lymphoma, bladder, esophagus, cervix uteri, liver, stomach, prostate, colorectum, breast and lung cancer. Furthermore, leukemia accounts for 2.5% of all diagnosed cancers in adults of both genders[1]. For children under the age of 15 years, the incidence of acute lymphoblastic leukemia (ALL) worldwide varies between 20-35 cases per million, whereas the incidence of ALL in Costa Rica, in Mexico City and in the Hispanic populations of the USA is greater than 40 cases per million[2]. T-cell ALL (T-ALL) is an aggressive cancer derived from the malignant transformation of T-cell precursors, and account for 25% of all ALL cases in adults[3] and 15% in children[4]. Historically, T-ALL patients have had a worse prognosis than other ALL patients[5]. T-ALL remains an important cause of morbidity in both children and adults; however, the etiology of this malignancy still remains elusive and is the object of intensive research[6]. One possible cause of T-ALL development are infections with the human T-cell lymphotrophic virus 1 (HTLV-1). It was the first discovered retrovirus and also the first one associated with a neoplastic malignancy. Recent studies show that ATL occurs in ~5 % of HTLV-1-infected individuals[7]. Although sporadic cases may occur, the majority of affected patients come from specific geographical areas (Japan, Caribbean basin, and Central Africa)[8]. However, this retrovirus is also related to many other diseases such as uveitis, Sjögren syndrome, polymyositis, synovitis, as well as some autoimmune diseases, like tropical spastic paraparesis and HTLV1-associated myelopathy[9]. Besides HTLV-1 infections, other related causes of T-ALL may involve parental exposure to chemicals such as benzene and other hydrocarbons like oil-based paint during pregnancy and in the postnatal stage, but the epidemiological evidence remains inconsistent and inconclusive[10]. Another important factor contributing to T-ALL

development is the accumulation of mutations in certain genes, as described in more detail below.

2.1.2 Disease origin

Currently, tumors are recognized as complex entities with phenotypic and genetic heterogeneity, not only within the primary tumor, but also within their metastases[11]. Two theories have been proposed to explain the intra-tumor heterogeneity: the clonal evolution or stochastic model, and the cancer stem cell (CSC) or hierarchical model[12,13]. Unlike the hierarchical theory of cancer development implicating CSC as the origin of acute myeloid leukemia (AML), the stochastic model has been suggested for B- and T-ALL development both in human and mouse[14–16]. The CSC model proposes that some cancers are organized into a hierarchy of subpopulations of tumorigenic cancer stem cells and their non-tumorigenic progeny (**Figure 1**).

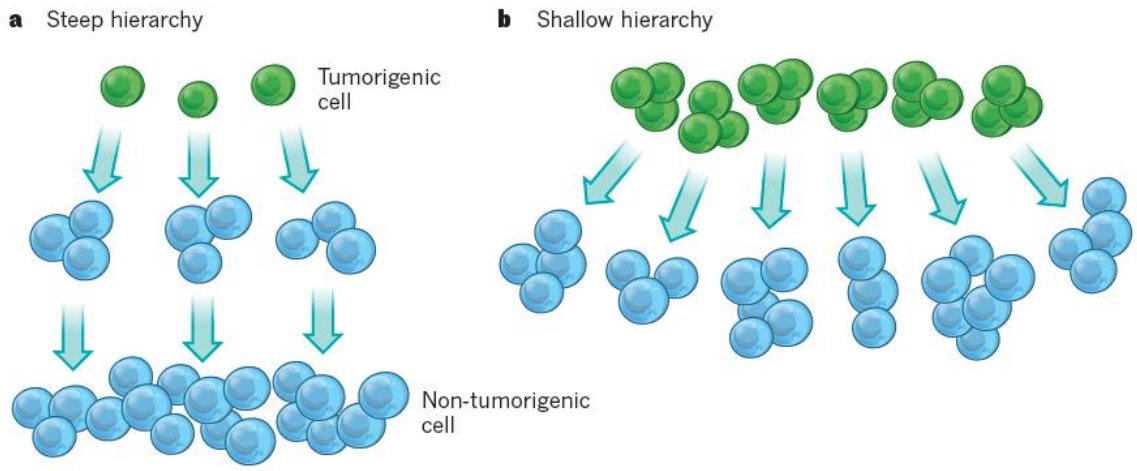

Figure 1. Cancers may have hierarchical organization in which subpopulations are arranged into TC and NTC. (***a***) Some hierarchies might be steep in which TC are rare but give rise to numerous NTC, (***b***) whereas other hierarchies might be shallow and TC are common but give rise to a small number of NTC. Also, cancers may have almost no hierarchy with very few NTC[13].

In these cases, CSC are thought to drive tumor growth and disease progression, perhaps through therapy resistance and metastasis[13]. Using transplantation assays to test the potential of cancer cells to form a tumor, several groups demonstrated the existence of phenotypically distinct subpopulations of tumorigenic cells (TC) and non-tumorigenic cells (NTC). In some cancers such as acute myeloid leukemia (AML)[17,18], chronic myeloid leukemia (CML)[19], breast cancer[20], glioblastoma[21], colorectal[22–24], pancreatic[25] and ovarian cancer[26–28], the fraction of cells that formed tumors were rare.

On the other hand, the clonal evolution theory proposed by Nowell in 1976 describes that a single cell gives rise to tumor growth through a continued accumulation of mutations, and where all cells within the tumor have the same potential to promote tumor growth (**Figure 2**).

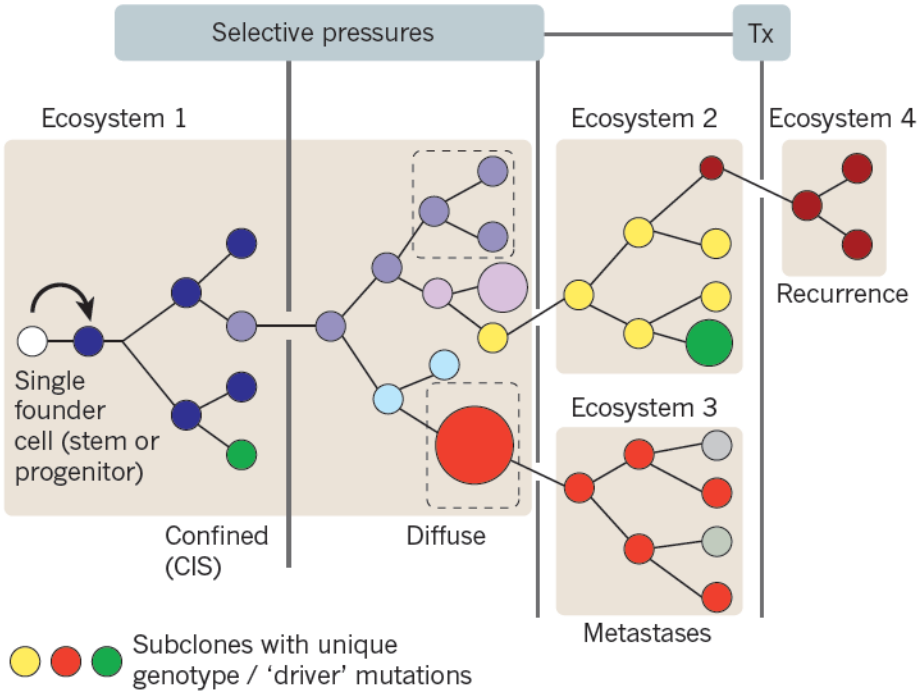

Figure 2. The branching architecture of cancer evolution. Scheme showing that cancer cell development follows Darwinian rules. Each colored circle stands for a different subclone. Ecosystems represent different tissues where some clones adapt and proliferate more than others. After selective pressures (vertical lines), some subclones acquire new mutations that contribute to its survival and proliferation[12].

The continuous change in the genome results in a sequential selection of diverse subpopulations with more aggressive phenotypes[29]. Each subpopulation can mutate independently contributing to intra-tumor heterogeneity[30]. Clonal evolution most likely proceeds via branching instead of a linear progression since branching generates greater clonal diversity, hence contributing to heterogeneity[31]. Furthermore, proliferation and drug resistance to a given drug follow Darwinian rules where the fittest clones will survive[12,32].

In ALL, this model describes various precursor differentiation stages of lymphocytes that may function as leukemia-initiating cells (LICs). LICs have features such as stemness, plasticity and the ability to create an irregular proinflammatory microenvironment in the bone marrow (BM) promoting leukemia progression at the expense of normal hematopoiesis[33–35]. However, the intricate multistep process by which cells are transforming to malignant cells remains to be completely deciphered. A handful of genes/pathways have emerged as playing prominent roles in the self-renewal of normal hematopoietic stem cells (HSCs) and LICs, including Notch1, Wnt and Sonic hedgehog[36]. It has been found that 70% of chromosomal translocations in childhood T-ALL involve genes belonging to oncogenic transcription factors with important regulatory activity in hematopoiesis[15]. It has also been shown that gain-of-function mutations in the oncogenes *SCL* (formerly known as *Tal1*)*, LMO1* and *NOTCH1* together with an active pre-T-cell receptor (TCR) were sufficient to induce transformation of susceptible T-cell progenitors[15]. Moreover, retroviral delivery of constitutively active Notch1 protein in HSCs exclusively induce T-ALL[37]. Genes encoding for *NOTCH1* and *CDKN2A/2B* are mutated in more than 50% of adult and childhood T-ALL cases. Also, a large variety of genes are mutated at lower frequency, but also contribute to the transformation of normal T cells into aggressive leukemia cells with impaired differentiation, improved survival and proliferation, and altered metabolism, cell cycle and homing properties[38]. Studies analyzing patients with *NOTCH1* mutations have shown that patients with additional mutations or deletions in the tumor suppresor *PTEN* gene, which causes aberrant phosphatidylinositol 3-

kinase (PI3K)-AKT signaling, have a poorer prognosis than patients carrying only *NOTCH1* mutations[39,40].

Based on stage-specific differentiation markers, disease-ALL can be sub-classified into early T-cell precursor ALL (ETP-ALL), cortical, and mature T-ALL. ETP-ALL is defined by the absence of CD4, CD8, and CD1a and frequent expression of one or more myeloid markers[41]. ETP-ALL show a block at the earliest stages of T cell differentiation ($CD4^-CD8^-$) and a transcriptional program related to that of the early T-linage progenitor cells, HSCs and myeloid progenitors. On the other hand, cortical T-ALLs with a $CD1a^+CD4^+CD8^+$ immunophenotype show a particularly favourable prognosis. The more mature late cortical thymocyte T-ALL displays a $CD4^+CD8^+CD3^+$ immunophenotype that is characterized by activation of the *SCL* oncogene[41]. Standard chemotherapy regimens result in remission in approximately 80% of pediatric and 45% of adult T-ALL patients, but not in ETP-ALL that has a higher rate of relapse, with a 10-year overall survival of only 19% compared to 84% for all other T-ALLs[42].

2.2 Novel treatment strategies for T-ALL

The survival of children with ALL has greatly improved over the last 40 years with rates of up to 80% among the main reference centers[43]. Nevertheless, relapse of ALL is still the main cause of treatment failure[44]. The majority of relapses occurs in the bone marrow (BM) alone or in combination with extramedullary sites, mainly central nervous system (CNS) or the testicles[45]. Extramedullary relapses have become greatly rare in clinical trials, yet, CNS relapse remains a major obstacle to curing ALL, accounting for 30% to 40% of initial relapses in some clinical trials (Pui CH. 2006). The development of new agents for the treatment of T-ALL has lagged behind the developments in B-ALL, where multiple antibodies have shown significant success (Kantarjian et al. 2012). The high frequency of *NOTCH1/FBX7* mutations in T-ALL implies a potential of these molecules for therapeutic targeting. Notch activation depends on proteolytic cleavage of cytoplasmic tail catalyzed by the γ-secretase complex, generating intracellular Notch1 (ICN)[46]. Then, ICN translocates to the nucleus and binds to Mastermind family proteins to form a large

transcriptional complex[47,48]. In preclinical models, inhibition of Notch1 receptor activation by γ-secretase inhibitors (GSI) resulted in G0/G1 cell-cycle arrest and decreased proliferation of T-ALL cells[46]. Moreover, targeted inhibition of JAK-STAT signaling with tyrosine kinase inhibitors such as tofacitinib has been proposed for the treatment of T-ALL with activating *JAK3* mutations[49]. Also, inhibition of the PI3K-signaling pathway using inhibitors of PI3K[50], AKT[51,52], mTOR[53] or dual PI3K-mTOR[54] offers an attractive therapeutic avenue with or without addition of glucocorticoids for the treatment of high-risk *PTEN*-null T-ALL cases[55]. Finally, preclinical evaluation of a BCL2 inhibitor, ABT-199, in a cell-line model of ETP-ALL, which is characterized by higher expression of BCL2, showed strong anti-leukemic effects and synergism with glucocorticoids (often included with other agents in cancer treatment although the mode of action is not clear[56], doxorubicin, and L-asparaginase[57,58]. Doxorubicin is a cytostatic drug widely used as chemotherapeutic agent in several types of cancers[59], while L-asparaginase is selectively used for ALL since leukemic cell production of L-asparagine (Asn) cannot keep up with its high demand. Thus, leukemic cell survival depends on Asn uptake from the diet[60]. Asparaginase catalyzes the conversion of Asn to aspartic acid and ammonia, thereby depleting serum Asn and starving leukemic cells of the Asn necessary for DNA, RNA, and protein synthesis leading ultimately to cell death[61].

2.3 Clinical manifestations and leukemic infiltration

Patients with ALL have several non-specific symptoms that include weight loss, fever, night sweats, fatigue and loss of appetite. Most signs and symptoms of ALL result from shortages of normal blood cells, which happen when the leukemia cells outgrow the normal HSCs in the bone marrow. These shortages show up on blood tests as anemia, they can also cause symptoms like weakness, airsickness, dyspnea, recurrent infections, bruising and bleeding such as frequent or severe nosebleeds and bleeding gums (American Cancer Society, 2016). T-ALL is an aggressive leukemia that can show leukemic and/or lymphomatous

manifestations[55]. Its clinical presentation can include hyperleukocytosis with extramedullary involvement of lymph nodes (LN) and other organs, frequently including infiltration of the CNS and the presence of mediastinal mass arising from the thymus[55]. The thymic enlargement may displace the trachea and esophagus causing cough, pain, dyspnea, or dysphagia, and may compress the mediastinal vessels leading to the life-threatening superior vena cava syndrome[6]. Some patients with CNS involvement present with cranial nerve deficits, symptoms of CNS hemorrhage, or symptoms of spinal cord compression. However, most patients with CNS leukemia have no clinical manifestations whatsoever[62]. Ocular involvement in patients with acute leukemias is common, occurring in 17% of childhood acute leukemia cases, while only 3.6% of the children were symptomatic[63]. Leukemic infiltration of testicles is a phenomenon which has posed some interesting and clinically important questions as there appears to be a wide variation in its incidence as reported in different ALL trials; also, it is uncertain whether testis is a sanctuary site which may require individual treatment[64]. In order to infiltrate different tissues, leukemic T cells must cross the vascular endothelial barrier, a process that requires transendothelial migration (TEM).

2.4 Normal and leukemic T-cell TEM

In response to inflammatory stimuli, leukocytes migrate from the blood into the tissues through several sequential adhesive steps[65]. This process termed leukocyte adhesion cascade is critical for fighting infections and wound healing and is thus indispensable for survival[66]. The general sequence of adhesive interactions of leukocytes with endothelial cells (EC) allows first tethering, rolling, and slow rolling, followed by firm adhesion, crawling, and transmigratory cup formation on the apical endothelial surface leading to diapedesis[66]. Tethering and rolling of leukocytes start with low-affinity interactions mediated by the endothelial adhesion molecules E- and P-selectin (CD62E and P, respectively) and their leukocyte counterparts L-selectin and P-selectin glycoprotein ligand-1 (PSGL-1)[67]. Next, leukocytes sense chemokines presented on EC that induce activation by

conformational changes of the integrins leukocyte function-associated antigen-1 (LFA-1) and very late antigen-4 (VLA-4). This enables them to interact with endothelial intercellular adhesion molecule-1 (ICAM-1) and vascular cell adhesion molecule-1 (VCAM-1), respectively, ultimately leading to firm adhesion and arrest of leukocytes on the endothelial surface[67] (**Figure 3**).

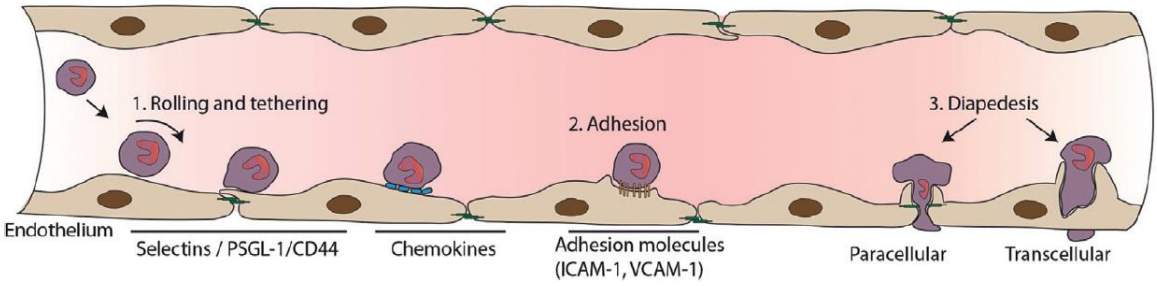

Figure 3. Schematic overview of the multistep paradigm of leukocyte TEM. Rolling and tethering allow leukocytes to recognize chemokines presented on the luminal side of the endothelium and these stimulate the activation of integrins leading to firm adhesion. Subsequently, leukocytes cross the endothelial barrier (diapedesis) either via the paracellular or the transcellular pathway[68].

Then, leukocytes crawl on EC to a suitable spot for TEM that can happen across the body of a single EC by transcytosis (called transcellular pathway, only 10% of TEM) or between the junctions of EC (called paracellular pathway, 90% of TEM)[69]. It is not entirely clear how leukocytes choose their TEM spot, but it has been described that endothelial junction strength and endothelial cell stiffness play a major role[70,71]. Molecular differences to the classical extravasation cascade that have been described for the extravasation of normal and leukemic T-cells are described in detail in the following chapters.

2.4.1 T-cell TEM

Among leukocytes, lymphocytes are remarkable cells regarding their migration potential, as they continuously recirculate in and out of lymphoid and non-lymphoid tissues throughout their life[72,73].

Moreover, each subpopulation of T-cells possesses different migration capabilities because of their surface receptor patterns, the state of activation, the vascular bed and the counterreceptors expressed on EC[66,74,75]. *In vitro* studies using human T-cells demonstrated that behavior of T cells is different from other leukocytes regarding TEM[66]. T cells adhere randomly to the endothelium and locomote on the EC surface allowing enough time to induce chemokine-chemokine receptor crosstalk necessary for T cell integrin activation and subsequent TEM[76]. Also, this contact time enables the T cell receptor (TCR) to recognize potential antigens presented on the surface of EC, a newly explored pathway to achieve TEM[77]. T cell extravasation involves a set of common and T cell-specific molecules that participate in the different steps of T cell recruitment[66] as described below.

Tethering and rolling

In search of specific antigens, naive lymphocytes continuously circulate through the body migrating from one lymphoid organ to another via the blood stream and the lymphatics[78]. Lymphocytes exit the blood stream within the LN via high endothelial venules (HEV), which are specialized post-capillary venules. The first step of T cell TEM in HEV is the capture and tethering of circulating lymphocytes (**Figure 4**)[78]. Transient interactions between HEV ECs and naïve lymphocytes are mediated by L-selectin (CD62L) expressed on the lymphocyte surface and sialomucins also called peripheral node addressins (PNAd) that are constitutively expressed on the HEV surface (such as GlyCAM-1, CD34, podocalyxin, endomucin, CD300g and mucosal addressin cell adhesion molecule-1 (MAdCAM-1))[73]. On the other hand, E- and P- selectin are induced on the EC surface in inflamed tissues and mediate capturing of lymphocytes from the blood stream with their respective T cell ligands PSGL-1 and L-selectin on lymphocytes resulting in rolling of T cells on the apical EC surface[79]. It is important to mention that although all T cells express PSGL1, only certain subsets of T cells (such as Th1) express the correctly glycosylated form of PSGL-1 capable of binding to selectins[80]. Thus, not all T cells rely on PSGL-1-mediated interactions to start TEM.

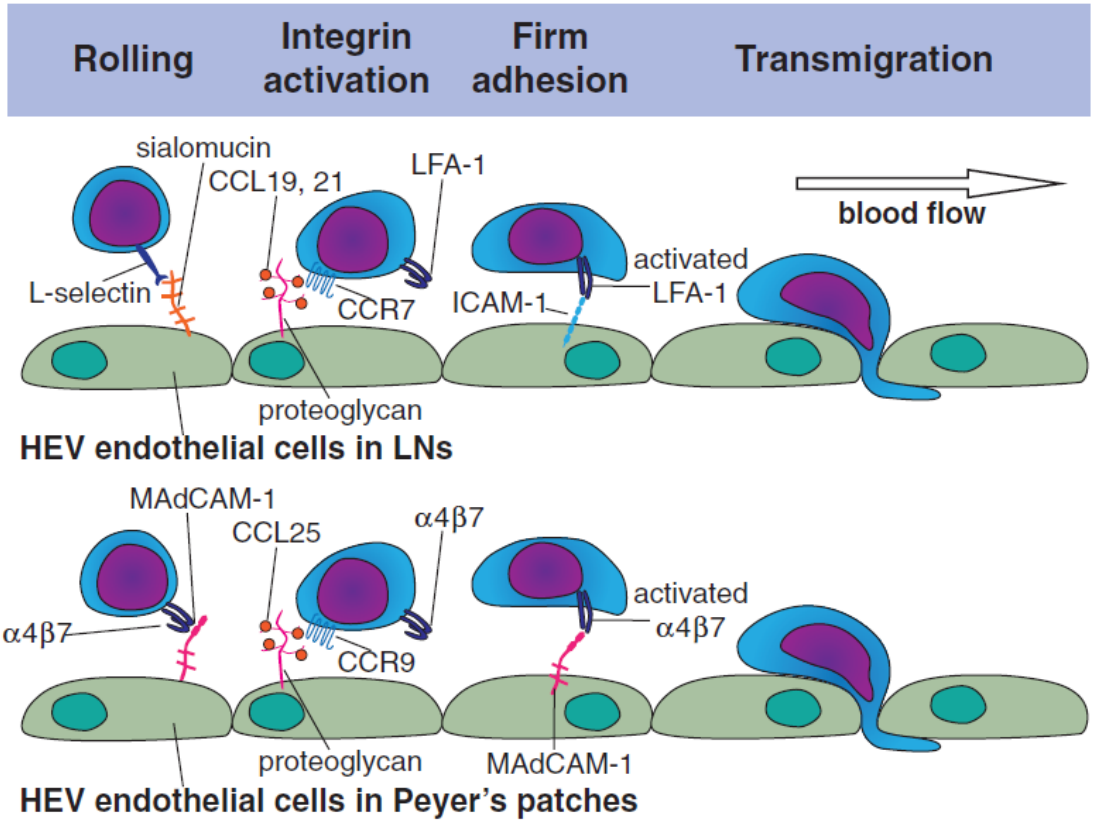

Figure 4. The lymphocyte adhesion cascade in the lumen of HEVs. In peripheral lymph nodes (LN), lymphocytes initiate rolling through L-selectin-sialomucin interactions. Subsequently, LFA-1 integrin on T cells is activated mainly after binding of CCR7 to the chemokines CCL19 and CCL21. T cells then bind to EC molecules such as ICAM-1 and VCAM-1 through activated LFA-1 and VLA-4, respectively, and proceed to migrate across the HEVs. By contrast, in HEVs of Peyer's patches, lymphocyte rolling is mediated by $\alpha_4\beta_7$-integrin-MAdCAM-1 interactions in response to CCR9 activation by CCL25[73].

Lymphocyte CD44, a molecule capable of binding to the extracellular matrix glycosaminoglycan hyaluronan as well as E-selectin, is important to slow down the rolling velocity[68]. *De novo* expression of E-selectin on microvascular EC is induced in response to cytokines such as IL-1, TNF-α, and other stimuli like bacterial lipopolysaccharide (LPS). On the other hand, P-selectin is stored in Weibel-Palade bodies that are rapidly mobilized to the plasma membrane of EC in response to mediators of acute inflammation[81].

Adhesion

Binding of selectins on T-cells stimulates “outside-in” signals, increasing the affinity of integrins such as LFA-1 and VLA-4[82], which mediate firm adhesion to EC adhesion molecules such as ICAM-1 (CD54), VCAM-1 and MAdCAM-1[78] (**Figure 4**). Integrins exist in three conformational states: a bent conformation that has a closed head piece and thus low affinity for its ligands, and two extended conformations with either closed (intermediate affinity) or open headpiece (high affinity) (**Figure 5**)[83].

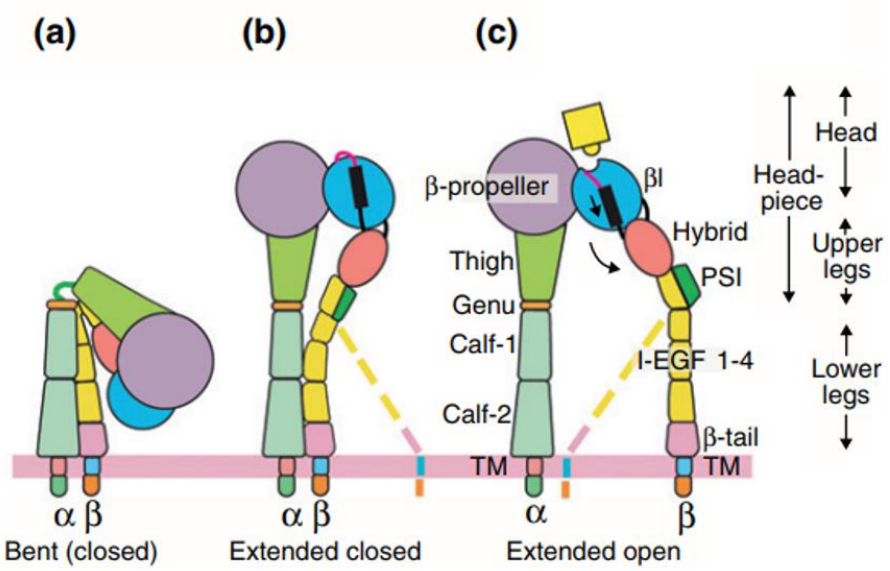

Figure 5. The integrin conformational states. In basal conditions, integrins are dynamically equilibrated in the three states. The bent-closed conformation (a) has low affinity; the extended-closed conformation (b) has intermediate affinity. The extended-open conformation (c) has high affinity for ligands. Conformational changes into the high-affinity form is commonly triggered by inflammation[83].

VLA-4 ($\alpha_4\beta_1$-integrin, a.k.a CD49d/CD29) belongs to a β1 integrin subfamily comprised of at least 6 members (VLA-1–VLA-6) with different α-chains associated with the β1 chain. They function as receptors for extracellular matrix proteins such as collagen, fibronectin, laminin and osteopontin (OPN), as well as for the EC adhesion molecules VCAM-1 and MadCAM[84,85]. VLA-4 plays major roles in tissue-specific migration of T-cells during inflammation and metastasis[86]. Also, VLA-4

activation (high-affinity conformation) in T cells is essential for VCAM-1 recognition on activated EC and subsequent TE [87]. Basal expression of ICAM-1 in EC is low, but it is highly upregulated during inflammatory processes via nuclear factor κB (NF-κB) (**Figure 6**)[88].

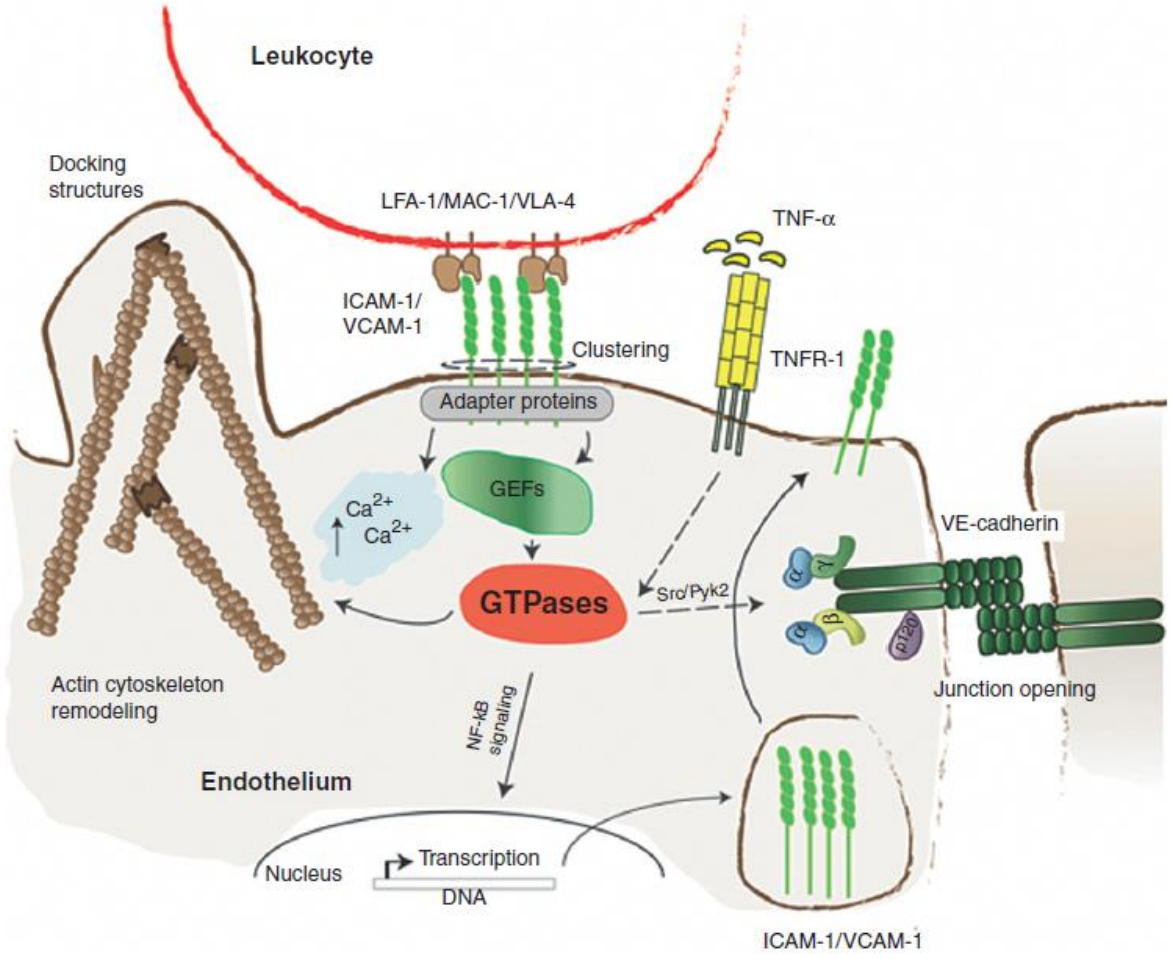

Figure 6. Endothelial pathways involving Rho-GTPases regulating leukocyte extravasation through the paracellular route. Clustering of ICAM-1 and VCAM-1 result in a cascade of signals that are initiated in the endothelium including increase of calcium levels, activation of small Rho-GTPases, actomyosin contractility and activation of kinases. Together this results in the transient opening of endothelial cell-cell juncions allowing leukocytes to cross paracellularly. In addition, clustering of ICAM-1/VCAM-1 can result in increased expression of ICAM-1 and VCAM-1; thus supporting a positive feedback loop to trigger leukocyte TEM[68].

VCAM-1 is absent in resting cells[89], and unlike ICAM-1, VCAM-1 expression depends on the expression and activation of the Rho-GEF Trio and its target Rac1, by directing translocation of the transcription factor Ets2 to the nucleus[88]. On the other hand, naïve T lymphocytes express CCR7 and CXCR4 chemokine receptors, which upon binding to their ligands CCL19, CCL21, and CXCL12, respectively, presented on the surface of EC increase integrin affinity via conformational changes by "inside-out" signals leading to lymphocyte arrest[66,82,90,91]. CXCL12 binding to its receptor CXCR4 promotes adhesion, polarization and chemotaxis of T cells[76]. After firm adhesion, naïve T lymphocytes start to crawl along the luminal surface of HEVs in a VLA-4- dependent manner[87], in search for a suitable site to transmigrate termed hot spots or "exit ramps"[92]. It is unclear what determines the exit ramps for T cells, however, for neutrophils an enrichment of adhesion molecules or chemokines around specific pericyte gaps[93], release of chemoattractans from leading neutrophils[94], or deposition of matrix fragments produced by neutrophil proteases as chemotactic fragments have been suggested[95].

Diapedesis

Arrested lymphocytes must cross the endothelial layer in order to get access to the tissue. In this process, T effector cells (T_{eff}) use molecules such as platelet/endothelial cell adhesion molecule-1 (PECAM-1), CD99 and LFA-1 which bind to PECAM-1 (hemophilic), CD99 (hemophilic) and ICAM-1/Junctional adhesion molecule-A (JAM-A) on endothelial cells (**Figure 7**), respectively[96]. These interactions mediate lymphocyte-EC contacts within the inter-endothelial space and induce sequential and reciprocal signaling[97].

2.4.2 Molecules involved in leukemic T-cell infiltration

Infiltration of the CNS is an important aspect of T-ALL pathophysiology[98]. However, the mechanisms that govern invasion of the CNS by T-ALL cells are not fully understood. It has been proposed that leukemic cells could enter the subarachnoid

space from the BM of the skull via the bridging veins or from the cerebrospinal fluid via the choroid plexus. Alternative routes may include invasion of the cerebral parenchyma via brain capillaries, or infiltration of the meninges via bone lesions of the skull[62]. Moreover, leukemic T cells infiltrate more frequently other organs such as skin, lung, and the gastrointestinal tract when compared with leukemic leukocytes of other hematopoietic malignancies[99].

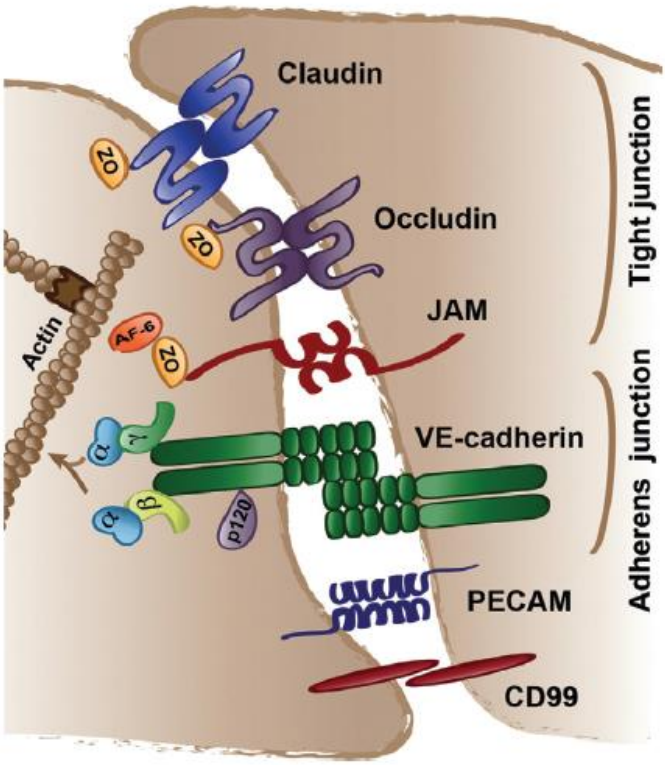

Figure 7. **Endothelial cell-cell junctions.** Adherens and tight junctions mediate endothelial cell-cell adhesion through specific adhesion molecules: VE-cadherin (AJ), claudin-5, occludin, and JAMs (TJ). These adhesion complexes are linked to the actin cytoskeleton through intracellular mediators: p120, α-, β- and γ-catenins and zona occludens (ZO) proteins. Moreover, PECAM-1 and CD99 contribute to endothelial cell-cell adhesion[68].

Patient-derived adult T-ALL cells adhered on IL-1β-treated HUVEC cells and antibody blockage of E-selectin completely inhibited T-ALL cell adhesion, whereas blockage of VCAM-1, LFA-1 or VLA-4 only partially inhibited adhesion suggesting

that binding of E-selectin with its counterreceptors PSGL-1, L-selectin, CD44 or CD43 initiates the firsts steps of TEM of leukemic T-cells[100]. T-ALL cells overexpress chemokine receptors such as CXCR4[101–103], CXCR7[104] and CCR7[103,105]. Pharmacological inhibition of CXCR4 in adoptive transfer experiments of T-ALL in NSG mice significantly reduced leukemic engraftment to BM and CNS involvement[98]. On the other hand, CXCR7 was shown to improve CXCL12-induced migration of T-ALL in *in vitro* models[104]. In addition, knock-down in animal models of either CCR7 or its ligand CCL19 specifically inhibited T-ALL cell infiltration to CNS[105]. Additionally, high levels of zeta-chain associated protein kinase 70 (ZAP-70), a tyrosine kinase from the Syk family constitutively expressed in T cells that mediates downstream signaling of pre-TCR and fully mature TCR[106], improved migration towards the chemokines CXCL12, CCL21 and CCL19 *in vitro*[103]. This phenomenon was mediated by ZAP-70 phosphorylation of extracellular signal-regulated kinase (ERK) that, in turn, induced up-regulation of CXCR4 and CCR7 expression. Moreover, high ZAP-70 levels in CNS infiltration of T-ALL patients samples positively correlated with high CCR7 and CXCR4 levels[103].

Stimulation of CXCR4 by CXCL12 in the BM is important for the maintenance of hematopoietic progenitors, as well as leukemic cell homing and stemness maintenance by positioning T-ALL cells in supportive niches of the BM[101]. Using *in vivo* imaging, T-ALL cells were found to be intimately in contact with CXCL12-producing vascular endothelial cells from BM[102]. Furthermore, conditional deletion of *Cxcr4* in murine T-ALL cells greatly reduced the overall number of T-ALL cells and suppressed the infiltration to BM, spleen, thymus and other organs[107]. *Cxcr4* deletion in T-ALL cells increased the survival of T-ALL cells in mice, even if *Cxcr4* was deleted after establishment of the disease suggesting a critical role for CXCR4 in the regulation of T-ALL LIC activity[102]. On the other hand, by using organoid-like 3-dimensional models (spheroids), it was shown that high CXCL12 levels on BM mesenchymal cells (MSC) ameliorated the proliferation of B-ALL cells, while, under inflammatory conditions established by B-ALL cells themselves, CXCL12 production by MSC diminished and promoted B-ALL proliferation[33]. Besides, calcineurin, a serin-threonine phosphatase, was found to be essential for T-ALL

maintenance and infiltration[108,109]. Calcineurin also regulates the expression of cortactin, an actin-binding protein (ABP) implicated in the regulation of the actin cytoskeleton and vesicle trafficking essential for CXCR4 surface expression[101]. However, the role of cortactin for infiltration of leukemic cells remains mostly elusive.

2.5 The actin-binding protein cortactin in cancer/leukemia

Cortactin is an ABP originally discovered as an 80/85 KDa substrate of Src kinase[110], that binds to actin structures at the cell cortex, hence its name [111]. Cortactin consists of four major domains: the N-terminal acidic (NTA) domain, 6.5 tandems repeat domain, a proline-rich domain and the C-terminal Src homology 3 domain (SH3 domain) (**Figure 8**)[112,113].

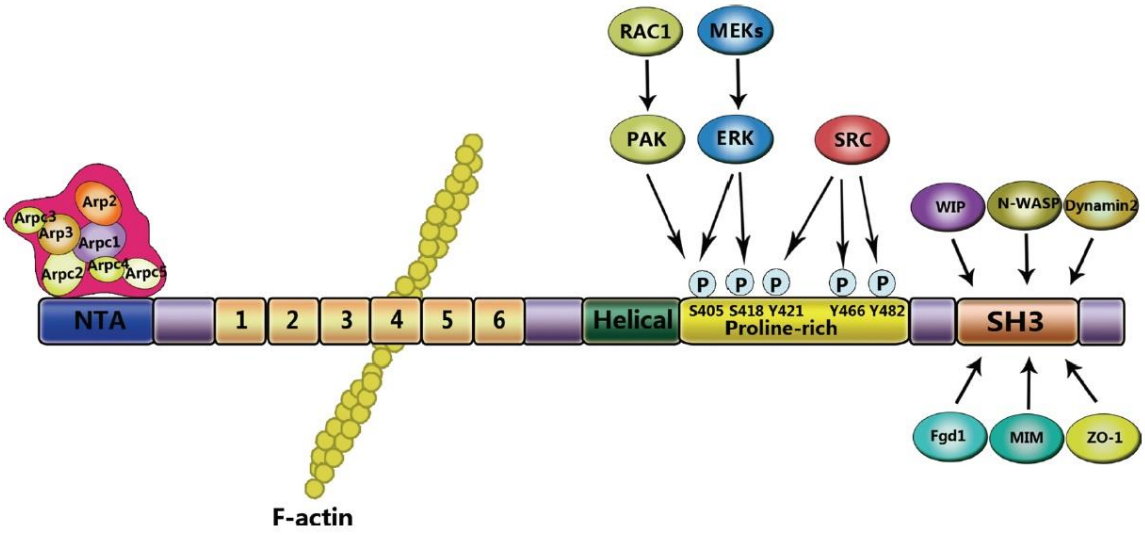

Figure 8. Structural domains of cortactin. Cortactin consists of distinct domains that interact with different molecules. The N-terminal acidic (NTA) domain is located at the N-terminus and interacts with the Arp3 subunit of the Arp2/3 complex. It has a 6.5 tandems repeat region domain which contains the binding site for F-actin. At the C-terminus, the proline-rich domain contains phosphorylation sites for serine- and tyrosine-kinases. The SH3 domain mediates the binding to cytoskeletal, membrane trafficking and signaling proteins[118].

The NTA domain contains a conserved aspartic acid, aspartic acid, tryptophan (DDW) motif which is required for the binding to the Arp3 subunit of the Arp2/3 complex[114]. Cortactin binds to the Arp2/3 complex but is by itself a weak activator of Arp2/3. However, it can recruit and increase the activity of other nucleation promoter factors (NPF) such as N-WASP[115]; and stabilize newly branched actin filaments. The NTA domain is followed by 6.5 37-amino-acid repeat domains that mediate F-actin binding. Essential for F-actin binding is the fourth repeat, whereas the third and the fifth repeats are essential for maintaining the binding efficiency[116,117]. Next is a proline-rich domain that is also enriched in serine, threonine and tyrosine residues that are susceptible to phosphorylation[112]. Finally, at the C-terminus, cortactin has a SH3 domain mediating interactions with several actin cytoskeleton effectors or scaffolding proteins[119,120]. Cortactin activity is strictly regulated by post-translational modifications such as serin/threonine and tyrosin phosphorylation and lysine acetylation[121]. Phosphorylation on serine 405 (S405) and S418 by ERK has been reported to recruit N-WASP, leading to actin polymerization mediated by the Arp2/3 complex[122]. Phosphorylation of tyrosine 421 (Y421) and Y470 by Src kinase is associated with lamellipodial protrusion and cell migration[123,124]. Furthermore, acetylation of cortactin (and deacetylation by histone acetyl transferase p300) diminishes the affinity to F-actin by neutralizing the positive charges of lysine residues, and reducing cell motility[125,126]. In addition, deacetylation mediated by histone deacetylase 6 (HDAC6) plays an important role in invasion of breast cancer cells[127]. Deacetylation of cortactin is also mediated by sirtuin-1[126].

Cortactin is encoded by the *cttn* gene (formerly called *EMS1*) located in the 11q13 region. Cortactin is ubiquitously expressed with the exception of some hematopoietic cells[128]. Two alternative splice variants of human cortactin have been identified, termed SV1 and SV2, that lack the 6th (exon 11) or the 5th and 6th (exon 10 and 11) repeats in the F-actin binding domain, respectively. Both splice variants behave like wt-cortactin with respect to subcellular localization and tyrosine phosphorylation. However, they differ significantly in their ability to induce

cell migration, to bind and cross-link F-actin, and to promote Arp2/3-mediated actin polymerization *in vitro*[129] (**Figure 9**).

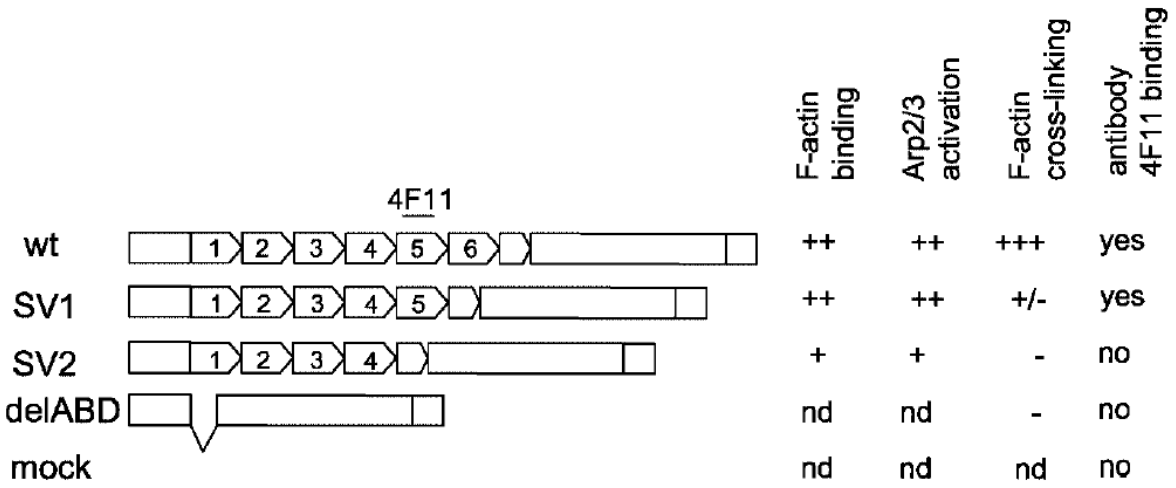

Figure 9. Schematic representation of the cortactin variants and their activities. For F-actin binding, ++ indicates a binding affinity of 0.4 µM, and + indicates 4 µM. For Arp2/3 activation, Arp2/3-mediated actin polymerization in the presence of wt-, SV1- or SV2-cortactin was monitored. The epitopes of the monoclonal antibody 4F11 used to detect cortactin in experiments are represented in the figure. delADB represents a modified protein lacking the actin binding domain. *nd,* not determined [129].

Cortactin has an essential role in human neoplasia. Cortactin expression is upregulated in several types of human solid cancers including head, neck and esophageal squamous carcinomas, colorectal carcinoma, gastric cancer, hepatocellular cancer, breast cancer and ovarian cancers[130–133]. Cortactin overexpression is frequently due to chromosomal amplification of the 11q13 region where the cortactin-encoding *cttn* gene is located, and associated with poor prognosis[131,134,135]. In solid tumors, cortactin has essential roles in invadopodia formation, cancer cell migration, and metastasis[121]. Recently, cortactin, which has until recently been considered absent in lymphocytes, was found overexpressed in B-cells of adult chronic lymphocytic leukemia (B-CLL). Of note, some of the B-CLL patients overexpressed the wt-cortactin of 80 kDa, which is usually completely absent in normal B cells from healthy donors. In addition, some B-CLL patients

expressed the SV1-cortactin isoform of 70 kDa, which is partially present in normal B cells, while others expressed both wt- and SV1-cortactin isoforms. Moreover, cortactin overexpression in B-CLL patients correlated with negative prognostic factors for CLL, such as ZAP-70 and CD38 overexpression[136]. Cortactin expression in B cells of CLL patients correlated with the release of matrix metalloproteinase 9 (MMP-9) and motility of neoplastic cells[137]. However, it is unknown whether leukemic T cells also express cortactin, and if so, what isoform. As high rates of infiltration during T-ALL is dependent on cytoskeleton rearrangement and transendothelial migration, processes known to be regulated by cortactin, it is tempting to speculate that leukemic T cells do express cortactin, and that cortactin expression could be related to the aggressiveness of T-ALL.

3. Justification

T-ALL accounts for 25% of leukemia cases in adults and 15% in children. It is an aggressive neoplasm due to its high infiltration to organs such as brain, lungs and testicles, and due to high relapse rates. Infiltration of T-ALL cells to extramedullary sites requires extravasation, a phenomenom highly dependent on actin cytoskeleton rearrangement. Cortactin is an ABP with an important role in cell adhesion and migration. High levels of cortactin correlate with invasiveness of solid tumors and recently, cortactin expression in B-CLL was related to an unfavorable prognosis. However, whether cortactin is expressed in T-ALL cells and correlated with high infiltration rates and aggressiveness remains elusive. Therefore, evaluating cortactin expression and its role in T-ALL cell migration might contribute to a better understanding of leukemic T cell invasion.

4. Hypothesis and Aims

4.1 Hypothesis

T-ALL cells that express high levels of cortactin possess an enhanced transmigratory ability.

4.2. General aim

To evaluate the expression of cortactin in the murine T-cell acute lymphoblastic leukemia cell line 6645/4, and its role in TEM and BM colonization.

4.2.1 Particular aims

1. To determine the immunophenotype of the murine T-ALL cell line 6645/4.
2. To compare expression of molecules needed for transendothelial migration between normal T cells and 6645/4 leukemic T cells.
3. To determine the expression of cortactin in 6645/4 before and after TEM.
4. To evaluate the correlation between cortactin expression and colonization of 3D stromal cell organoids by 6645/4 leukemic T cells.

5. Materials and Methods

5.1 Materials

5.1.1 Reagents

Chemicals	Company
$Na_2HPO_4•7H_2O$	J.T. Baker #3824-01
$KH_2PO_4•3H_2O$	Macron #7088-04
NaCl	J.T. Baker #3624-05
KCl	J.T. Baker #3040-01
$CaCl_2$	J.T. Baker #1313-01
$MgSO_4•7H_2O$	Merck #A999986
$NaHCO_3$	Sigma #S5761-1KG
$CuSO_4•5H_2O$	Sigma #C3036-250G
NaF	Sigma #S7902
Na_3VO_4	Sigma #S6508
Hydrochloric acid	J.T Baker #9535-05
Acetic acid glacial	J.T Baker #9508-05
Sodium hydroxide	Macron #7708-10
EDTA	Sigma #E9884-500G
HEPES	Biowest #P5455-100GR
D-glucose	Macron #4912-12
Tris•base	J.T. Baker #4109-06
Glycine	J.T. Baker #4059-06

Glycerol	Sigma #G6279-500ML
Ammonium persulfate	BioRad #161-0700
30% Acrylamide/bis solution	BioRad #161-0153
TEMED	BioRad #161-0801
β-Mercaptoethanol	Sigma #-M3148-25ML
Tween® 20	Sigma #P1379-500ML
Triton™ X-100	Sigma #T9284-500
Nodinet™ P-40	Sigma #21-3277 SAJ
Sodium dodecyl sulfate (SDS)	BioRad #1610302
Skim milk	Svelty
Bovine serum albumin	Sigma #A2153-100G
Complete protease inhibitor cocktail	Roche #11697498001
Methyl alcohol	J.T. Baker #9070-03
Ponceau S	Merck-Millipore #159270025
Ethyl alcohol	Sigma #E703-1L
ANESKET® (Ketamine)	PiSA #Q-7833-028
PROCIN® (Xylazine)	PiSA #Q-7833-099
MEM NEAA 100X	Gibco #11140-050
Antibiotic Antimycotic 100X	Corning #30-004-Cl
L-glutamine 100X	Gibco #A2916801
Na-pyruvate 100X	Gibco #11360-070
Fetal bovine serum	Biowest #S1810
ECGF from bovine pituitary	Sigma #E0760-15MG
Murine SDF-1α (CXCL12)	PreproTech #250-20A-10UG

Tylosin	Sigma #T3397-20ML
Gentamicin sulfate	Calbiochem #345814
Agarose	Cleaver Scientific Ltd #CSL-AG500
Gelatin	CTR Scientific
Accutase®	Sigma #A6964-100ML
Trypsin-EDTA 0.25%	Sigma #T4049-500ML
TrypLE™ Express	Gibco #12604-013
Collagenase from *Clostridium histolyticum*	Sigma #C0130
Ficoll-Paque™ PLUS	GE Healthcare #17-1440-03
BD Pharm Lyse™	BD Biosciences #555899
Saponin	Sigma #84510-100
Hoechst33342	Sigma #B2261

Antibodies	**Company**
Anti-γ tubulin	ThermoFisher Scientific #MA1-850
Anti-CD11a, clone M17/4	Kindly provided by Dr. Vestweber, MPI Münster, Germany
Anti CD-31 (PECAM-1)	Santa Cruz Biotechnology #sc-376764
Anti-CD54 (ICAM-1), clone YN1/1.7.4	Kindly provided by Dr. Vestweber, MPI Münster, Germany
Anti-CD106 (VCAM-1), clone 6C7.1	Kindly provided by Dr. Vestweber, MPI Münster, Germany
Anti-cortactin Alexa Fluor® 488 conjugated, clone 289H10	Kindly provided by Dr. Rottner, TU Braunschweig, Germany
Alexa Fluor® 488 goat anti-mouse IgG (H+L)	Life Technologies #A11001
Alexa Fluor® 488 goat anti-rat IgG (H+L)	Invitrogen #A11006
Alexa Fluor® 488 rabbit anti-rat IgG (H+L)	Invitrogen #A21210

Alexa Fluor® 565 rabbit anti-mouse IgG (H+L)	Life Technologies #A27023
Anti-cortactin (p80/85) Alexa Fluor® 488 Conjugated, clone 4F/11	Millipore #16-228
APC anti-mouse CD45	BioLegend #103112
APC Rat Anti-Mouse CD62L	BD Pharmigen™ #553152
APC anti-mouse CD184 (CXCR4)	BioLegend #146507
APC/Cy7 anti-mouse CD45	BioLegend #103116
APC/Cy7 anti-mouse Ly-6A/E	BioLegend #108126
FITC anti-mouse CD45	BioLegend #103108
HS1 (Rodent-Specific) Rabbit Ab	Cell Signaling #4557S
Pacific Blue™ anti-mouse CD45	BioLegend #103126
Pacific Blue™ anti-mouse H-2Kb	BioLegend #116514
PE anti-mouse CD3	BioLegend #100206
PE anti-mouse CD4	BioLegend #100408
PE anti-mouse CD8	BioLegend #100708
PE anti-mouse CD29	BioLegend #102208
PE anti-mouse CD45	BioLegend #103106
PE/Cy5 anti-mouse CD45	BioLegend #103110
PE/Cy5 anti-mouse CD117 (c-Kit)	BioLegend #105810
TruStain fcX™ (anti-mouse CD16/32)	BioLegend #101320
Mouse Anti-rabbit IgG-HRP	Santa Cruz Biotechnology #sc-2357
Goat anti-mouse IgG-HRP	Santa Cruz Biotechnology #sc-2005
Dynabeds® Sheep anti-Rat IgG	Invitrogen #110.35

Kits	Company
BD Cytofix/Cytoperm™	BD Biosciences #554714
DC™ Protein assay	BioRad #5000112
MojoSort™ Mouse CD3 T Cell Isolation	Biolegend #480024
CellTrace® Cell Proliferation Kit (CFSE, DMSO)	Invitrogen #C34554
SuperSignal® WestFemto	ThermoFischer Scientific. #34095

Culture mediums	Company
Dulbecco Modified Eagle's Medium (DMEM) - high glucose	Sigma #D5648-10X1L
Iscove's Modified Dulbecco's Medium (IMDM)	Sigma #I7633-10X1L
RPMI-1640 Medium	Sigma #R4130-10X1L
Minimum Essential Medium Eagle	Sigma #M4655-1L

Buffers	Composition
PBS 1X	138 mM NaCl 3 mM KCl 8.1 mM Na_2HPO_4 1.5 mM KH_2PO_4 pH 7.4
PBS-EDTA	PBS 1X 5 mM EDTA
TBS 1X	150 mM NaCl 10 mM Tris•base pH 8.0
TBS-T	TBS 1X 0.1% Tween® 20
HBSS 1X	8000 mg/L NaCl

	400 mg/L KCl 40 mg/L Na_2HPO_4 60 mg/L KH_2PO_4 350 mg/L $NaHCO_3$ 1000 mg/L D-glucose pH 7.4
HBSS Ca^{+} Mg^{2+}	HBSS 1X 140 mg/L $CaCl_2$ 120 mg/L $MgSO_4$
Mg^{2+} lysis buffer 1X	25 mM HEPES pH 7.5 150 mM NaCl 10 mM MgCl2 1 mM EDTA 1 % NP-40 2 % glycerol Complete protease inhibitor cocktail
5X Laemmli buffer	0.1875 M Tris-HCl pH 6.8 45% glycerol 2.5% SDS 1.78 M β-mercaptoethanol 0.00125% bromophenol blue
SDS-PAGE buffer	25 mM Tris 192 mM glycine 0.1% SDS pH 8.3
Transfer buffer	20% methanol 25 mM Tris 192 mM glycine 0.1% SDS
Blocking buffer	TBS-T 5% BSA or skim milk
MojoSort™ Buffer 1X	PBS 1X 0.5% BSA 2 mM EDTA pH 7.2

5.2. Methods

5.2.1 Cell culture

The murine leukemic T cell line 6645/4 (T cell acute lymphoblastic leukemia, with constitutive expression of the oncogenes SCL and LMO1), kindly provided by Dr. Peter Aplan (NIH, Bethesda, MA), was cultured in IMDM medium supplemented with 20% fetal bovine serum (FBS), 1% L-glutamine, 6 mg/mL HEPES, 4.5 mg/L D-glucose and 1% antibiotic/antimycotic[138]. MS5 stromal cells[139] and OP9-GFP stromal cells (ATCC CRL-2749) were cultured in MEM supplemented with 10% FBS and 1% antibiotic/antimycotic. bEnd.5 cells were kindly provided by Dr. Vestweber (MPI, Münster, Germany) and cultured in high-glucose DMEM supplemented with 10% FBS, 2% L-glutamine, 1% Na-pyruvate, 1% MEM NEAA and 1% antibiotic/antimycotic. 6C7.1 hybridoma (kindly provided by Dr. Vestweber, MPI, Münster, Germany) were cultured in DMEM supplemented with 10% FBS, 2% L-glutamine, 1% Na-pyruvate, 1% MEM NEAA, 1% antibiotic/antimycotic and 50 µM β-mercaptoethanol. M17/4 hybridoma (kindly provided by Dr. Vestweber, MPI, Münster, Germany) were cultured in RPMI-1640 supplemented with 10% FBS, 2% L-glutamine, 1% antibiotic/antimycotic and 50 µM β-mercaptoethanol.

5.2.2 Production of hybridoma supernatants containing monoclonal Abs

First, to verify whether 6C7.1 and M17/4 hybridoma cells are producing antibodies, a small fraction of hybridoma culture was grown in a T25 flask containing 7 mL of serum-free medium and incubated at 37°C for 7 days. Hybridomas are partially adherent, trypsin was used to completely detach cells. Then, the medium was centrifuged to remove debris, and the supernatant was collected. Supernatant from hybridomas were analyzed by 8% SDS-PAGE and Coomassie staining of the gel to visualize the 56 and 25 KDa bands, corresponding to the heavy and light chains of the produced antibodies, respectively. If positive, hybridomas were cultured in complete medium in a T25 flask until confluence. Subsequently, hybridoma

cultures were centrifuged and supernatants discarded. Hybridoma cells were resuspended in T125 flasks containing 500 mL of serum-free medium, and incubated at 37°C for 7 days. Finally, supernatants containing the monoclonal antibody were centrifuged to remove cellular debris, and stored with 0.04% NaN3 at 4°C. Supernatants were analyzed again by SDS-PAGE to assure antibody production.

5.2.3 Mice

The Institutional Animal Care and Use Committee (IACUC) of CINVESTAV approved all animal studies. Mice were kept in the animal facility of CINVESTAV. Mice were euthanized by cervical dislocation. All mice used during this work were 6-8 week old male C57BL/6 wild-type mice.

5.2.4 Isolation and cultivation of murine lung endothelial cells (MLEC)

One day before murine lung endothelial cells (MLEC) isolation, anti-PECAM-1 antibodies were coupled to magnetic beads coated to anti-rat secondary antibodies. Briefly, 40 µL of Dynabeads® (10^7, sheep anti-rat) were washed with 1 mL of PBS containing 0.1% BSA using a magnetic separator. Then, the beads were washed again and resuspended in 200 µL of PBS+0.1% BSA. Subsequently, 30 µL of rat anti-mouse PECAM-1 (CD31, clone MEC 13.3, 0.5 mg/mL, BD #553370) were added to the magnetic beads and incubated overnight at 4°C in an overhead rotator. The next day, magnetic beads were washed three times with MLEC media, and finally resuspended in 200 µL MLEC media.

To obtain MLEC, one mouse was anesthetized with an overdose of ketamine/xylazine. Then, the peritoneal and thoracic cavity were opened, and the peritoneal organs were moved aside to have optimal access to heart and lungs. The mouse was perfused by injecting PBS into the right heart chamber until lungs

appear white. The lungs were cut free of large blood vessels or extracellular matrix and placed in a sterile 2 mL Eppendorf tube containing 1mL of MLEC media (DMEM+20%FBS+1%L-glut+1%AA+5µg/mL ECGF) with 1mg/mL Collagenase from *Clostridium histolyticum*. Lungs were cut and homogenized with sterile sharp scissors for around 15 minutes, and incubated in a 37°C water bath for 1.5 hours with occasional gentle mixing. Next, the cell suspension was passed through a 40 µm cell strainer into a 50 mL falcon tube. The strainer was washed with 10 mL of MLEC media, the cell suspension was centrifuged for 5 min at 1200 rpm without brake to assure proper pelletation, and the supernatant was carefully removed. Cells were resuspended in 1 mL of MLEC media, transferred to a 1.5 mL Eppendorf tube containing 100 µL of anti-PECAM1-coated magnetic beads and incubated for 45 min at 4°C in an overhead rotator. Next, the tube was placed in the magnetic separator at 4°C for 3 min to assure complete magnetic adhesion of the cell-carrying beads. The supernatant was removed, and cells were washed two times with 1mL of MLEC media. Finally, sorted cells were resuspended in 1 mL of MLEC media and were plated into two TPP® 6-well plates containing 2 mL of pre-warmed MLEC media. Media was replaced after 24 hours.

To propagate and maintain MLEC, medium was aspirated and cells were washed two times with 2 mL of sterile pre-warmed PBS. Then, 2 mL of trypsin-EDTA 0.25% were added to the plates and cells were incubated at 37°C until detached. Then, 2 mL of complete medium was added to each plate to inactivate trypsin, and the cell suspension of one dish was plated into three TPP® T25 flasks containing 4 mL of fresh MLEC medium.

5.2.5 Isolation of primary T cells from mice using the MojoSort™ negative CD3 isolation kit

Isolation of T cells was performed from spleen of 6-8 week male C57BL/6 mice. Mice were anesthetized with a cocktail of ketamine/xylazine, and sacrificed by cervical dislocation. The peritoneal cavity was opened and the spleen removed

using sharp scissors and forceps, and placed in 1 mL of cold PBS+3%FBS. Then, the spleen was disaggregated mechanically, using a syringe plunger by grinding the tissue through a 40 µm cell strainer into a 50 mL falcon tube and washing with cell strainer with PBS+1%FBS. Subsequently, the cell strainer was washed with 10 mL of PBS+1%FBS. The cell suspension was centrifuged for 5 minutes at 1500 rpm, then supernatant was discarded. Cells were washed with 10 mL MojoSort™ 1X buffer and counted using a Neubauer chamber. Cell numbers were adjusted to a concentration of 10^7/100 µL. Next, 100 µL of cell suspension (10^7 cells) were transferred to a 5 mL polypropylene tube, and 10 µL of the Biotin-Antibody Cocktail containing Biotin anti-Ly6G/Ly6C (Gr-1), CD45R/B220, CD49b, CD19, CD11b, TER-119/Erythroid antibodies were added and mixed 10 s by vortexing. After 15 minutes of incubation in ice, 10 µL of Streptavidin-coated magnetic nanobeads were added and mixed for 10 s by vortexing. After another 15 min incubation in ice, 2.5 mL of MojoSort™ 1X buffer were added to the tube, mixed, and the tube was placed in the magnet for 5 minutes to allow magnetic attachment of cells bound to the beads. Finally, the suspension containing purified CD3 T cells was transferred into a new sterile polypropylene tube. Then, the magnetic separation step was repeated to increase the yield, and the suspension was transferred into a new sterile polypropylene tube.

5.2.6 RNA isolation

Total RNA was isolated from 6645/4 cells. $1x10^6$ cells were lysed in 200 µL of TRIzol reagent (Life technologies, USA) by vortexing for 1 min. Then, 40 µL of chloroform were added and the suspension was mixed gently by inversion, followed by a 3 min incubation at RT. Next, the mix was centrifuged for 30 min at 13,000 rpm at 4°C. Subsequently, the aqueous phase was carefully recovered and mixed gently with 100 µL of 2-propanol in a new 1.5 mL Eppendorf tube, and incubated overnight at 4°C. The next day, the mix was centrifuged for 30 minutes at 13,000 rpm at 4°C. The supernatant was discarded and the pellet was washed twice with 700 µL of 70% ethanol (in 0.1% diethyl pyrocarbonate [DEPC] water, as

RNase inhibitor). Then, the supernatant was discarded and the pellet dried at RT. Finally, the pellet was resuspended in 0.1% DEPC water, and RNA concentration was quantified using a Nanodrop 2000 (Thermo Scientific, Waltham MA, USA).

5.2.7 cDNA synthesis

0.1-5 µg of total RNA was used for cDNA synthesis. RNA was mixed with 1 µL of oligo $(dT)_{18}$ primer brought to a final volume of 11 µL with nuclease-free water, mixed gently, centrifuged and incubated at 65°C for 5 minutes in order to dissipate secondary structures of RNA. Then, the sample was incubated on ice, followed by a brief spin, and incubated again on ice for 2 min. Next, 4 µL of 5X reaction buffer, 1 µL of RiboLock RNase Inhibitor (20 U/ µL), 2 µL of 10 mM dNTP mix and 2 µL of M-MuLV Reverse Transcriptase (all from ThermoScientific) were added to each sample in a final volume of 20 µL. The mixture was gently mixed and centrifuged. Then, cDNA synthesis was performed for 60 min at 37°C in a 96-well thermal cycler (Applied Biosystems)

5.2.8 End-point PCR

Expression of the oncogenes SCL and LMO1 were analyzed using the primers described in Table 1. The PCR reaction mix was prepared as follows: 1X PCR buffer, 2.5 mM $MgCl_2$, 0.2 mM dNTPs, 0.2 µM forward primer, 0.2 µM reverse primer, 20 ng cDNA and 0.05 Taq polymerase enzyme in a final volume of 20 µL with molecular biology grade water. Amplifications were performed in a thermocycler using the following conditions: denaturation for 3 min at 95°C, followed by 30 cycles of 30 s at 94°C, 30 s at 60°C and 30 s at 72°C followed by 5 min at 72°C for a final extension for SCL amplification. For LMO1, denaturalization was for 3 min at 95°C; followed by 30 cycles of 30 s at 94°C, 30 s at 63°C and 30 s at 72°C followed by 3 min at 72°C for a final extension. PCR amplicons were analyzed in a 1.5% agarose gel for 30 min at 100 V.

Table 1. Primer sequences used for PCR of SCL and LMO1 oncogenes.

Gene	Amplicon length		Primer sequences
SCL	400 pb	Forward	5'-GCT CCT ACC CTG CAA ACA GA-3'
		Reverse	5'-GGC ATA TTT AGA GAG ACC G-3'
LMO1	197 pb	Forward	5'-AAG TGT GCG TGC TGT GAC TG-3'
		Reverse	5'-GCG AAG CAG TCG AGG TGA TA-3'

5.2.9 Transmigration assays

For transmigrations assays, 5 µm polycarbonate membrane Transwell® (Corning) filters were treated with 100 µL of sterile 0.1% gelatin for 30 minutes at room temperature. Then, gelatin was carefully removed and $3x10^4$ MLEC or bEnd.5 in 100 µl of complete medium were added on top of the transwell, and 600 µL of complete medium to the bottom well. As a control, $3x10^4$ MLEC or bEnd.5 in 100 µl of complete medium were cultured in a 96-well tissue culture plate coated with 0.1% gelatin to monitor confluency. Then, MLEC or bEnd.5 were incubated at 37°C until confluence (seen in the control culture on the 96-well tissue culture plate under a microscope). Once confluent, the medium was removed from the transwell and replaced with $5x10^5$ leukemic T cells 6645/4 in 200 µL of complete medium. The medium from the bottom well was also replaced with IMDM medium containing 100 ng/mL of CXCL12 as a chemotactic gradient. Subsequently, transwells were incubated for 3 hours at 37°C to allow transmigration [101]. After incubation, transwells were removed from the plate and medium from the bottom well was recollected in 1.5 mL Eppendorf tubes and centrifuged at 1500 rpm for 5 minutes. Next, the supernatants were discarded, and pellets of transmigrated cells were resuspended in 100 µL fresh medium. Subsequently, live transmigrated cells were

counted after trypan blue (1:1) staining in a Neubauer chamber and cortactin expression was measured by flow cytometry in both transmigrating and non-transmigrating cells as described below.

5.2.10 Spheroid co-culture assays

To allow OP9-GFP or MS5 cells to form spheroids, a round bottom 96-well plate was coated with 100 µL hot 0.1% agarose solution. Then, $2.5x10^4$ stromal cells/100 µL of Minimum essential medium supplemented with 10% FBS and 1% antibiotic/antimycotic were added to each agarose-coated well and incubated at 37°C for 24 h or until formation of the spheroid as seen under microscope at 40X objetive. Incomplete spheroids were discarded after 72 hours. Subsequently, $2.5x10^4$ Hoechst33342-stained 6645/4 leukemic T cells in 100 µL of IMDM supplemented with 20% FBS, 1% L-glutamine, 6 mg/mL HEPES, 4.5 mg/L D-glucose and 1% antibiotic/antimycotic, were added to each spheroid and co-cultured for 24 h to allow for spheroid colonization. After 24 hours, spheroids were removed from wells by pipetting up and down to resuspend it until spheroid was in the pippete tip. Then, spheroid was transferred with the minimum amount of volume to a well containing 100 µL of PBS-EDTA solution and by pipetting up and down any leukemic cell attached to the spheroid surface was removed. Next, spheroids were transferred to a well containing 100 µL of TrypLE™ Express reagent (Gibco) to disaggregate them, with concomitant pipetting up and down until obtaining a single cell suspension. Cell suspensions were passed through a 40-µm cell strainer to remove any clusters or fibers and collected in fresh 5 mL (12 x 75 mm) polypropylene tubes. Cells were stained using anti-mCD45 antibody to detect hematopoietic cells and cortactin; and analyzed by flow cytometry.

5.2.11 Immunofluorescence microscopy

6645/4 or normal T cells were fixed in 4% paraformaldehyde, and non-specific binding sites were blocked with PBS containing 5% BSA for 1 h. Slides were

incubated overnight at 4°C with primary unlabeled anti-cortactin (clone 289H10) and rodent-specific anti-HS1 (CellSignaling Technologies) antibody (diluted 1:100 for cortactin and 1:200 for HS1) in PBS 1% BSA. Next day slides were washed three times with PBS and incubated for 1 h at RT with conjugated Alexa Fluor® 565 goat anti-mouse secondary antibody for cortactin and Alexa Fluor® 633 goat anti-rabbit. Slides were examined, and images were taken using a confocal laser-scanning microscope (Leica TCS SP-8, Wetzlar, Germany).

5.2.12 Flow cytometry analysis of non-adherent cells

6645/4 leukemic T cells or purified normal T cells were stained with APC-CD62L (L-selectin), APC-CD184 (CXCR4), PE-CD29 (VLA-4), PE-CD3, PE-CD4 and PE-CD8 conjugated antibodies, and primary unlabeled antibodies against HS1 and cortactin and secondary Alexa Fluor® 488-coupled goat anti-rabbit and goat anti-mouse antibodies, respectively. All primary antibodies were at a 1:100 dilution, except for HS1, which was used at a 1:200 dilution. Secondary antibodies were used at a 1:1000 dilution. 6645/4 leukemic T cells were also stained with DNA-dyes Hoechst33342 (1:200) to identify cells. Acquisition was performed in a Beckman Coulter CytoFLEX LX cytometer, and data was analyzed using FlowJo X software.

5.2.13 Flow cytometry analysis in adherent cells

MLEC, bEnd.5, OP9-GFP, or MS5 cells were detached from flasks with Accutase® or TrypLE™ Express to preserve surface protein integrity. Cell suspensions were passed through 40 µm cell strainers and transferred to fresh 5 mL polypropylene tubes. Cells were incubated for 30 minutes with 300 µL of supernatants from YN1.1 or 6C7.1 hybridoma cultures containing rat monoclonal antibodies against CD54 (ICAM-1) and CD106 (VCAM-1), respectively. Next, cells were washed with PBS + 3% FBS, and subsequently incubated for 30 minutes with 1:1,000 dilution of secondary Alexa Fluor® 488 goat anti-rat IgG (H+L). Acquisition was performed in

Beckman Coulter CytoFLEX LX cytometer, and data was analyzed using FlowJo X software.

5.2.14 Western blots

Cell Lysis

Cells were lysed with Mg^{2+} lysis buffer (25 mM HEPES, 150 mM NaCl, 10 mM $MgCl_2$, 1 mM EDTA, 1% NP-40 and 2% glycerol), supplemented with 10 mM NaF, 1 mM Na_3VO_4 and 5X complete protease inhibitor cocktail, and three pulses of sonication (10 seconds, 40% amplitude). Then, lysates where centrifuged at 14,000 rpm for 10 min at 4°C, the supernatants were collected in a new 1.5 Eppendorf tube and protein concentration was quantified using the DC protein assay. After quantification, supernatants were mixed with 5X Laemmli buffer to a 1X concentration, boiled 5 minutes at 95°C to denature proteins and stored at -80°C until further use.

Protein quantification

The commercial kit DC Assay Method (BioRad, CA, USA) was used according to the manufacturer's instructions to quantify protein concentrations in cell lysates. Briefly, samples, diluent and reagents where prepared as follows: diluent was prepared by mixing the lysis buffer in deionized water in a 1:50 dilution; Reagent A' (RA') was prepared by diluting 1:50 Reagent S in reagent A, both provided with the kit. Samples were prepared by mixing 1 µL of the lysates with 19 µL of diluent. Then, the standard curve with Bovine γ-globulin (BGG) was pipetted in a 96-well plate, as indicated in Table 2. Standard curve and samples were prepared in triplicates.

Table 2. DC Assay Method standard curve reaction.

BGG standard curve					
1	**2**	**3**	**4**	**← Reaction order**	
Diluent	**BGG stock (1mg/mL)**	**Reactive A'**	**Reactive B**	**Final volume reaction**	**Final concentration**
20 µL	0 µL	10 µL	80 µL	100 µL	0 µg/µL
19 µL	1 µL	10 µL	80 µL	100 µL	1 µg/µL
18 µL	2 µL	10 µL	80 µL	100 µL	2 µg/µL
17 µL	3 µL	10 µL	80 µL	100 µL	3 µg/µL
16 µL	4 µL	10 µL	80 µL	100 µL	4 µg/µL
15 µL	5 µL	10 µL	80 µL	100 µL	5 µg/µL
14 µL	6 µL	10 µL	80 µL	100 µL	6 µg/µL
13 µL	7 µL	10 µL	80 µL	100 µL	7 µg/µL
12 µL	8 µL	10 µL	80 µL	100 µL	8 µg/µL

Afterwards, the plate was incubated in the dark for 15 minutes with gentle agitation. Then, absorbance was read at λ_{720nm} using a 96-well plate spectrophotometer (Tecan, Männedorf, Switzerland). To obtain protein concentration, the BGG standard curve was analyzed by linear regression and absorbances of samples were extrapolated using Graph Pad Prism 5 software.

SDS-PAGE

Equal protein amounts were loaded on an 8% SDS-PAGE. Separation was performed at 100 V for 2 h at RT. Gels were then washed with deionized water and equilibrated for 15 minutes in cold transfer buffer.

Blotting

Gels were placed in direct contact with nitrocellulose membranes and assembled in the cassette for blotting in cold transfer buffer for 90 min at 200 mA. After blotting, membranes were washed with deionized water and stained with Ponceau red to confirm protein transfer. Ponceau red was completely washed away with

TBS-T. Next, membranes were blocked with TBS-T containing 5% BSA for 1 h and incubated overnight at 4°C with purified anti-cortactin antibody (clone 289H10, 1:4,000) , rodent-specific anti-HS1 (1:200) or anti-γ tubulin (1:4000) as loading control. Subsequently, membranes were washed three times for 10 minutes with TBS-T buffer before incubation with secondary goat anti-mouse HRP or mouse anti-rabbit HRP (1:4000) antibodies for 1 h at RT. Again, membranes were washed three times for 10 minutes with TBS-T buffer.

Membrane imaging

Bands were revealed with SuperSignal® WestFemto chemiluminescent substrates. Chemiluminescence signals were recorded on a Chemidoc imaging system using Image Lab software (BioRad, California, USA).

Band intensity quantification

Band intensities were quantified using Image J software. Data was reported as relative pixel intensity obtained by dividing the pixel intensity of cortactin by the pixel intensity of tubulin of each sample.

5.2.15 Statistics

Graph Pad Prism 5 software was used to perform statistical data analysis. Differences between two groups were analyzed by Student's T-test, considering statistically significant values of $p<0.05$.

6. Results

6.1 Immunophenotype of the leukemic T cell line 6645/4

First, we analyzed the expression of the transgenic oncogenes SCL and LMO1 to corroborate that the cell line has maintained its leukemic phenotype. Using RT-PCR, we detected the expected amplicon of 197 base pairs (bp) corresponding to LMO1 mRNA, however, no SCL mRNA (400 bp) expression was detected (**Figure 10**). However, SCL expression data needs to be taken cautiously, as for the moment we do not have a positive control to verify SCL primer functionality. Nevertheless, it has been reported that some of the leukemic cell lines generated with these transgenic oncogenes loose the expression of either one or both oncogenes due to genetic events, while maintaining the leukemogenic potential[138]. In addition, LMO1 expression is sufficient to induce development of T-ALL[140]. Thus, the 6645/4 cell line has most likely conserved its leukemic phenotype, which nevertheless needs to be proven in transplantation assays in vivo, which are currently under way.

Since leukemias usually arise from immature hematopoietic cells, we determined the maturation stage of 6645/4 cells by analyzing the expression of CD44 and CD25, as well as CD3, CD4, CD8 expression. According to CD44 and CD25 levels, the 6645/4 cell line was in the double negative-3 (DN3) stage ($CD44^{-}CD25^{+}$) of T cell maturation (**Figure 11**). Furthermore, this cell line expressed CD3; but had low levels of CD8, and were negative for CD4 (**Figure 12**). Hence, the cell line 6645/4 appears to have an immature phenotype due to the lack of expression of CD4 and CD8, similar to what has been reported for ETP-ALL[41]. However, further studies with more markers will be needed to confirm this.

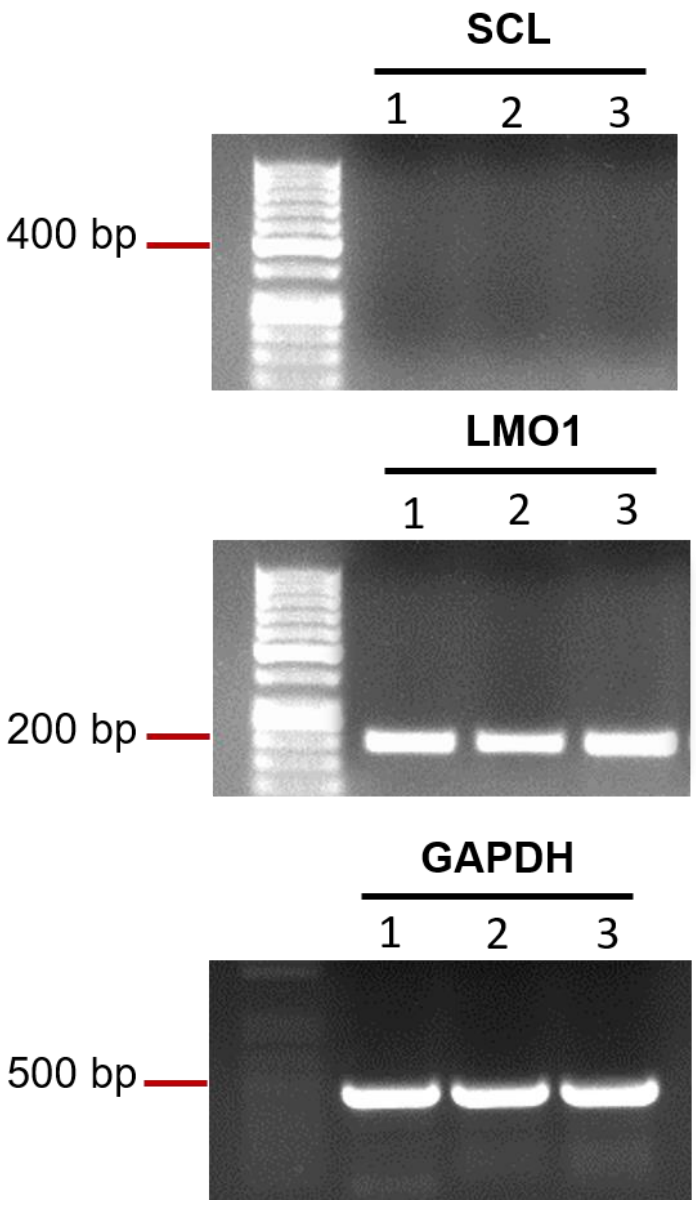

Figure 10. RT-PCR to analyze the expression of SCL and LMO1 in the 6645/4 cell line. Triplicates of cDNA obtained from 6645/4 total RNA were analyzed by PCR for the presence of SCL (400 bp) or LMO1 (197 bp) mRNA using specific primers. GAPDH mRNA (497 pb) expression was analyzed to verify cDNA integrity. PCR products were analyzed in a 1.5% agarose gel.

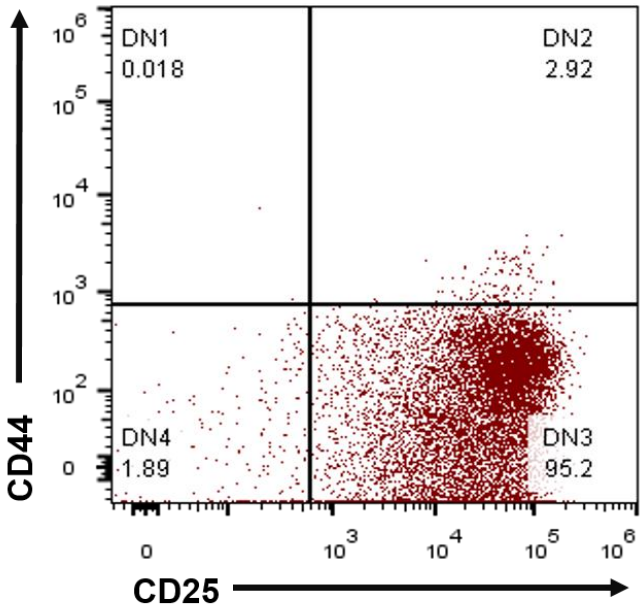

Figure 11. 6645/4 cells are in DN3 stage. A representative plot of CD44 and CD25 expression in 6645/4 cells is shown (n=3). Data was analyzed using FlowJo X software.

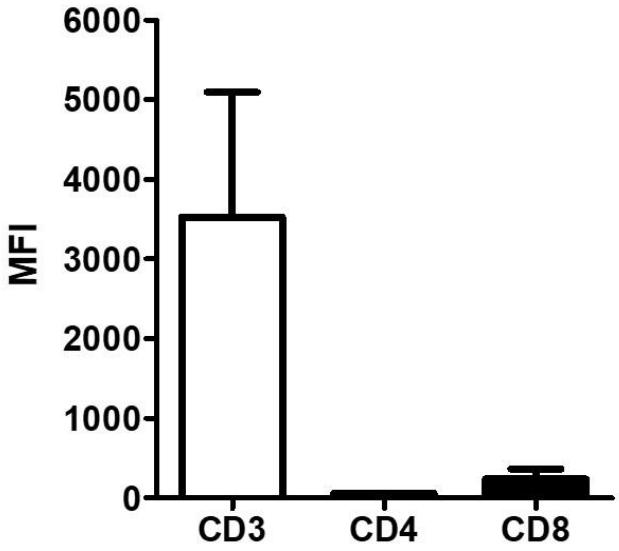

Figure 12. 6645/4 cells highly express CD3, but not CD4 or CD8. Each staining was performed independently three times. Data is displayed as mean fluorescence intensities (MFI) ± SD. FlowJo X software was used to analyze data. n=3

6.2 6645/4 leukemic cells express higher levels of CD3, VLA-4, cortactin, HS1 and CXCR4 than normal T cells

T-ALL is characterized by its high rates of infiltration[22,42,57,58,98,141]. Therefore, we analyzed the 6645/4 cell line by flow cytometry for the expression of adhesion molecules needed for transmigration such as CD62L, and CD29, and the chemokine receptor CXCR4. We found that 6645/4 cells showed a 20-fold increase in the expression of the chemokine receptor CXCR4 when compared to normal T cells. We also found that expression of the integrin VLA-4 was 4-times higher in 6645/4 cells. L-selectin expression was 28 times lower in leukemic T cells compared to normal T cells (**Figure 13**).

Given the recently described overexpression of cortactin and HS1 in B-CLL [136] and preB-ALL[142] cells, and their relevance for normal leukocyte transmigration, we analyzed their expression in the 6645/4 cell line. We saw a 5-fold increase in the expression of cortactin compared to normal T cells, whereas HS1 expression was only increase 1.2-fold (**Figure 13**). Since cortactin was correlated with extramedullary infiltration in preB-ALL[142], we next focused on evaluating the functional relevance of cortactin in this cell line.

6.3 6645/4 cells and normal T cells express the 80 KDa cortactin WT variant

It has been reported that expression of different variants of cortactin occurs in leukemias. For example, the 70 KDa SV1-cortactin variant was reported to be present in B-CLL patient samples[136], whereas the 60 KDa SV2-cortactin variant was present in preB-ALL patient samples[142]. Thus, we determined the expression of cortactin by WB. Lysates from 6645/4 leukemic and normal T cells showed that both cell types expressed only the 80 kDa WT isoform of cortactin (**Figure 14**).

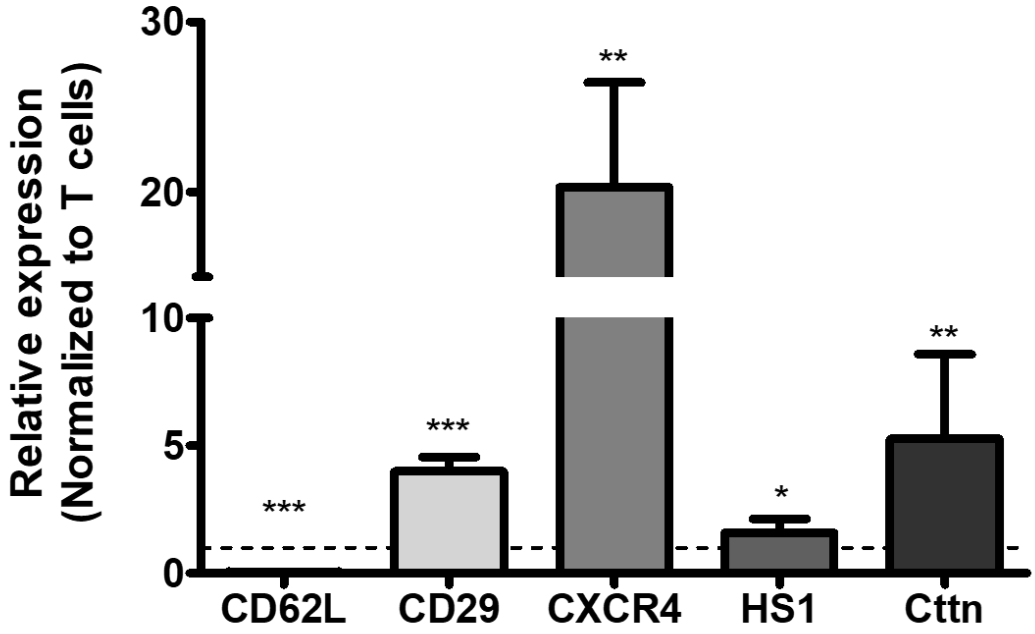

Figure 13. Expression of proteins needed for transendothelial migration in 6645/4 and normal T cells. Each staining was performed independently three times. Normal T cells were obtained from mouse spleens using the MojoSort CD3 magnetic isolation kit. Data are displayed as MFI ± SD normalized to the expression of each molecule in normal T cells (set to 1, dotted line). FlowJo X software was used to analyze data. Statistical significance was determined using unpaired Student's t-test. *p<0.05, **p<0.01, ***p<0.0001.

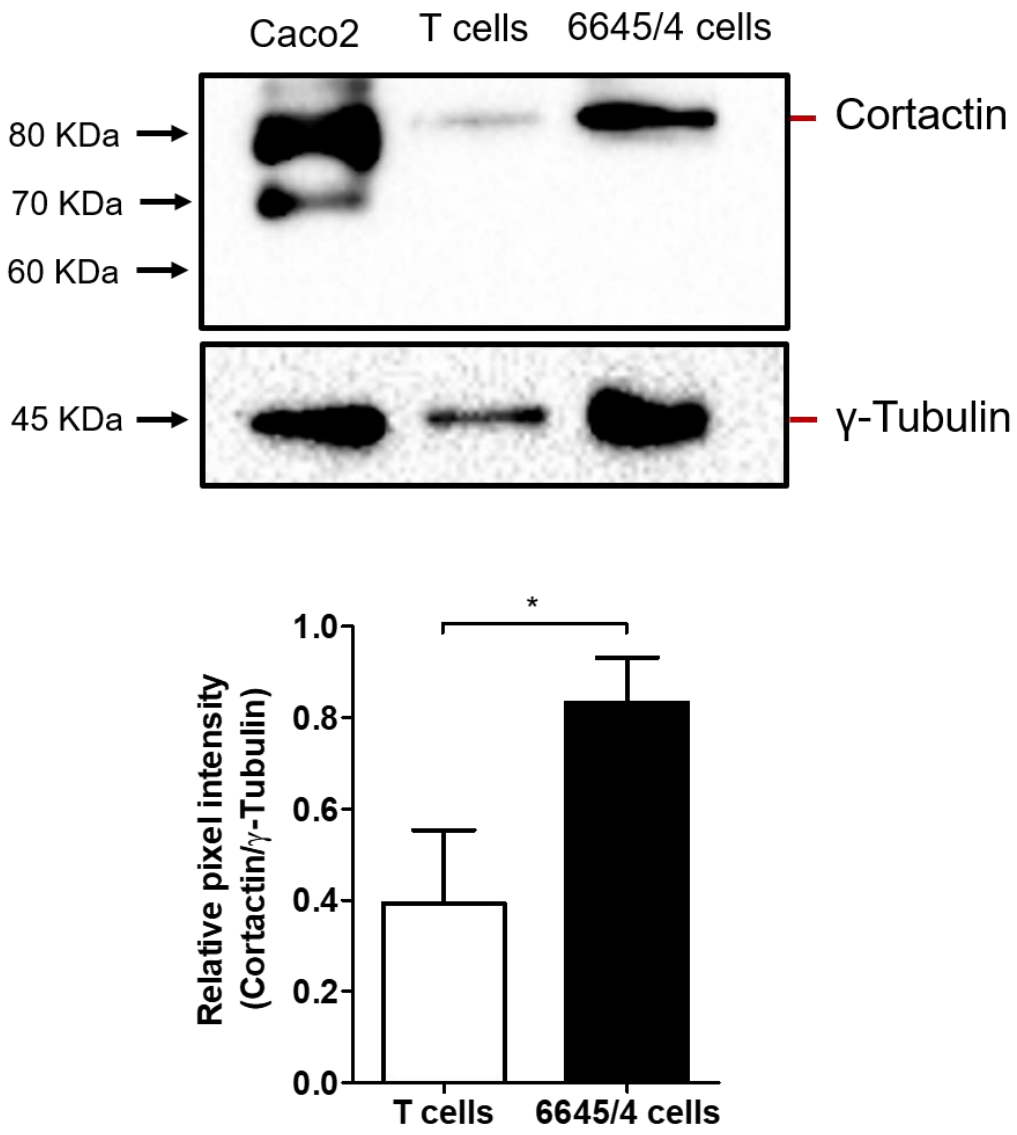

Figure 14. Leukemic 6645/4 cells and normal T cells express only the 80 KD wt-cortactin variant. Cortactin expression was determined by Western blot using lysates from 6645/4 leukemic T cells and normal T cells purified from mice spleens. Caco-2 epithelial cells served as control for cortactin expression (70 and 80 KDa). γ-Tubulin served as loading control. A representative blot of 3 independent experiments is depicted (upper panel). Densitometric analysis was performed using Graph Pad Prism 5 software. Statistical significance was determined using paired Student's t-test. Data are represent as mean relative pixel intensity ± SD. n=3. *p<0.05.

6.4 Cortactin and HS1 are enriched in the periphery of 6645/4 cells

In order to identify the cellular localization of cortactin and its homologue HS1, we performed immunofluorescence stainings in 6645/4 cells, and in normal T cells as control. Cortactin and HS1 partly co-localized in the cytosol and at the cell periphery of 6645/4 cells. In agreement with the previous data, cortactin expression was low in normal T cells, but it also did co-localize with HS1 (**Figure 15**).

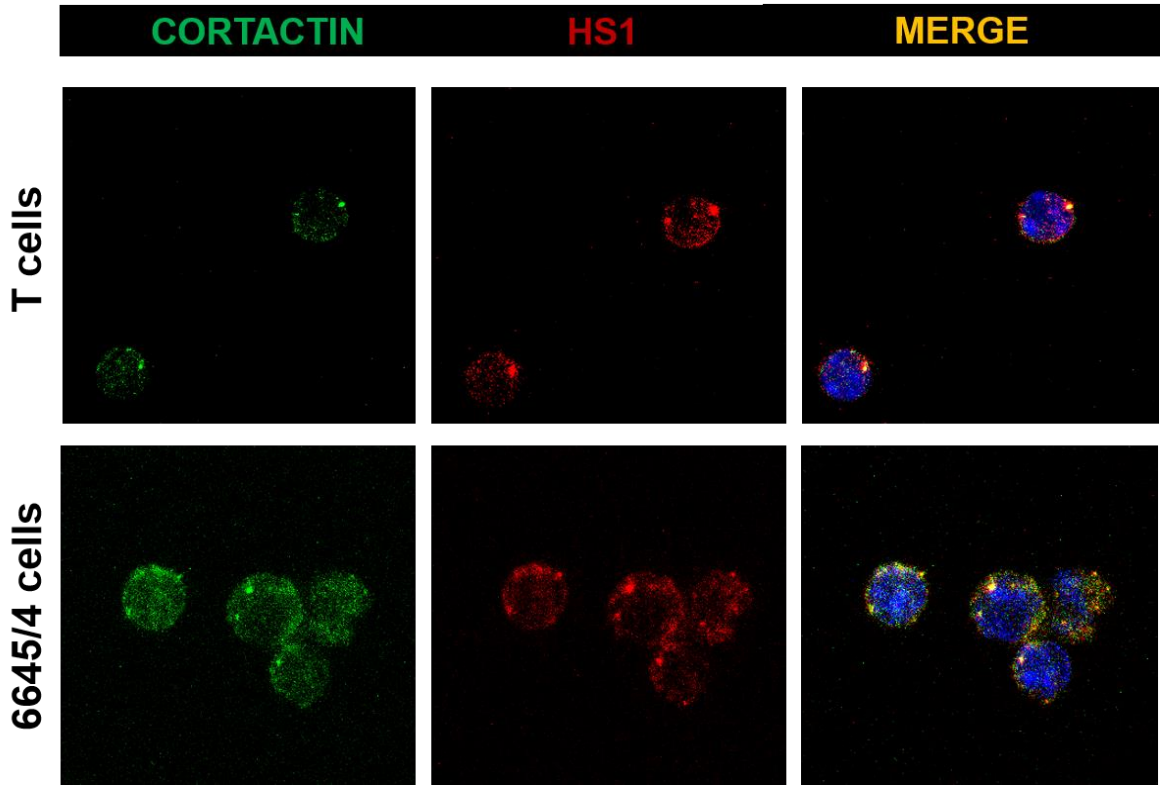

Figure 15. Localization of cortactin and HS1 in 6645/4 cells and normal T cells. 6645/4 and T cells were adhered to a poly-L-lysine-treated slide, fixed and stained for cortactin (green), HS1 (red) and DNA (DAPI, blue). Co-localization of cortactin and HS1 in the cytosol of both cell types can be observed, although cortactin expression is apparently stronger in 6645/4 cells in agreement with our flow cytometry and WB data. Representative images of 3 independent experiments are shown.

6.5 High cortactin expression levels in 6645/4 leukemic T cells is related to transendothelial migration advantages

The 6645/4 cell line expresses high levels of the molecules needed to accomplish transendothelial migration. Therefore, we evaluated the transmigratory potential *in vitro* compared to normal T cells. We found that 2.5% of 6645/4 leukemic cells are able to transmigrate *in vitro* through bEnd.5 monolayers towards a CXCL12 gradient (**Figure 16a**). Normal T cells had a lower rate of transmigration through bEnd.5 cells, where only approximately 1% of total applied cells were able to transmigrate (**Figure 16b**). Of note, transmigration was independent of previous endothelial activation with TNF-α. We also evaluated expression of endothelial adhesion molecules, since these molecules are essential for leukocytes to firmly adhere to the endothelium and subsequent transmigration. While basal ICAM-1 expression was high, VCAM-1 expression was low on bEnd.5 (data not shown). Thus, this finding might explain the overall low transmigration rate across bEnd5 cells, as T cell migration mainly relays on VLA-4/VCAM-1 interactions [87]. Thus, we will in the future repeat TEM assays using different endothelial cells such as primary murine lung endothelial cells.

Since cortactin has been implicated in the infiltration of leukemic cells[142], we evaluated the expression of cortactin in transmigrated and non-transmigrated cells. We found that transmigrated 6645/4 cells consistently had significantly higher levels of cortactin when compared to non-transmigrated cells (**Figure 17**). The same pattern was seen in normal T cells, where cortactin expression was also higher when they managed to transmigrate. Of note, the cortactin levels in normal T cells were significantly lower compared to 6645/4 cells, both in transmigrated and non-transmigrated cells (**Figure 17**). Furthermore, cortactin expression of transmigrated T cells did never even reach the levels of cortactin in non-transmigrated 6645/4 cells. Taken together, these results suggest a potential role of cortactin in the transmigration of leukemic cells, since the higher the cortactin expression is, the higher the transmigration rate.

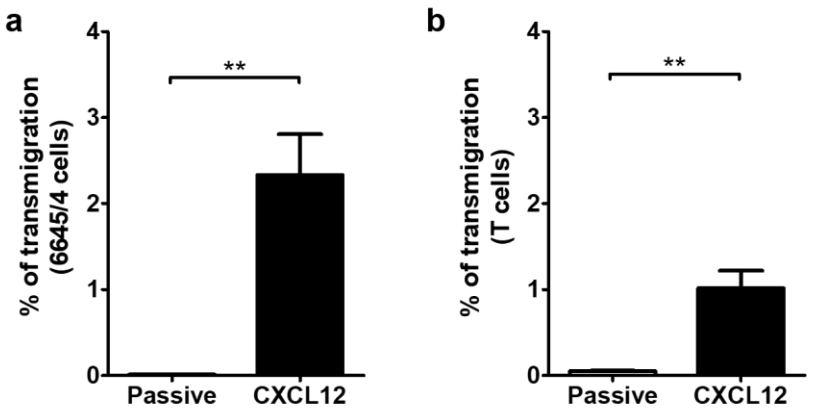

Figure 16. Transmigration assays with 6645/4 leukemic T cells through bEnd.5 endothelial monolayers. 5x10^5 T cells were placed in the upper chamber of Transwell filters containing bend5 monolayers; and transmigrated cells towards a CXCL12 gradient were recovered from the bottom chamber after 3 hours. a) Percentage of transmigration of leukemic T cells. b) Percentage of transmigration of purified normal T cells. Data are represented as mean % of transmigration ± SD. Unpaired Student's t-test was performed to determine statistical significance. n=3. **p<0.01.

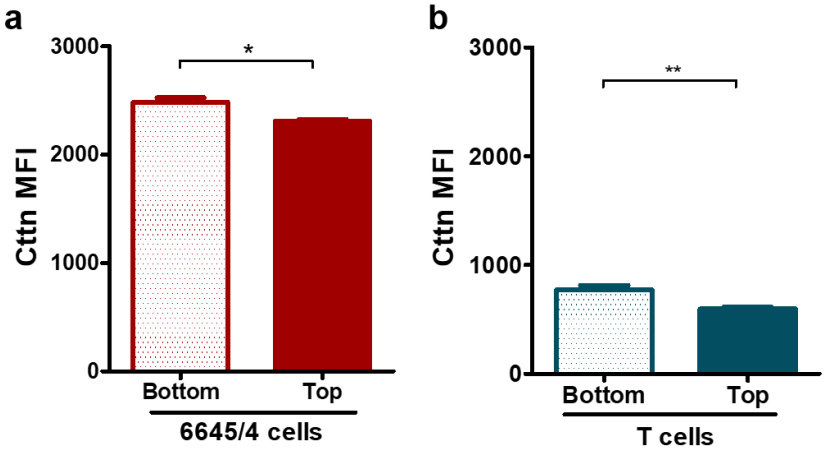

Figure 17. Transmigrated cells express higher levels of cortactin than non-transmigrated cells. Transmigrated 6645/4 cells (a) or normal T cells (b) were recovered after 3 h from the bottom chamber (bottom) and cortactin expression was analyzed by flow cytometry and compared with non-transmigrated cells recovered from the top of the monolayer (top). Data are depicted as mean fluorescence intensities (MFI) ± SD. Paired Student's t-test was performed to determine statistical significance. n=6. *p<0.05, **p<0.01.

6.6 High cortactin levels correlates with bigger size in 6645/4 cell line

Due to high levels of cortactin in transmigrated cells, we asked whether cortactin^{high} cells already exist as a subpopulation within the 6645/4 cell culture or if transmigration induces cortactin expression. For answer this question, we analyzed the expression of cortactin in 6645/4 cells again under basal conditions. We found no important differences in MFI of cortactin in these cells (not shown). However, when we analyzed cortactin vs forward scatter (FSC) we distinguished a clearly distinct population of cortactin^{high} cells that correlated with a bigger size (**Figure 18**). Thus, we analyzed separately the MFI of cortactin and FSC in cortactin^{high} cells, and then compared it with the population of 6645/4 cells showing lower cortactin expression. We found a significant 1.56-fold increase of cortactin levels and a significant 1.5-fold increase in average size. Thus, 6645/4 cells are heterogenous containing a population of cells with higher basal expression of cortactin and bigger size that might be the population with better transmigratory abilities. However, no report currently exists describing an association of cortactin overexpression with bigger cell size. Thus, more studies are needed to corroborate a possible relationship between cortactin, cell size and TEM.

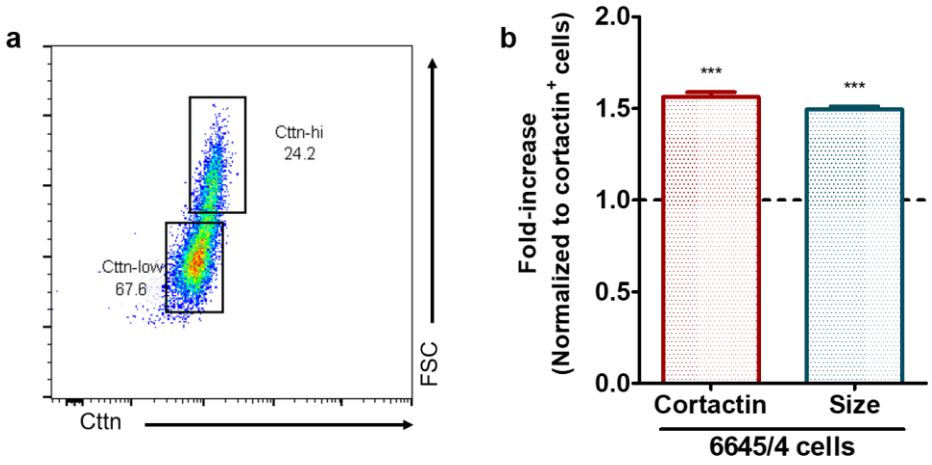

Figure 18. Cortactin^{high} 6645/4 cells are bigger than cortactin^{low} 6645/4 cells. (a) A representative dot-plot of cortactin expression in 6645/4 cells is shown (n=12). (b) Data are depicted as fold-increase ± SD normalized to cortactin^{low} 6645/4 cells (set to 1 dotted line). Paired Student's t-test was performed to determine statistical significance. ***p<0.0001

6.7 6645/4 leukemic T cells that colonized bone marrow stromal spheroids expressed higher levels of cortactin than those that stayed outside

Bone marrow colonization is a common trait of leukemias, as they establish themselves in normal niches and grow at the expense of normal hematopoiesis. Thus, we wanted to know whether high expression of cortactin in 6645/4 leukemic T cells correlates with colonization of spheroids of stromal cells resembling BM[33]. Leukemic T cells were stained with Hoechst33342 in order to trace them. After 24 hours of co-culture, cells inside and outside the spheroid were analyzed for expression of cortactin. We found that cells inside the spheroid had higher levels of cortactin when compared with cells outside (**Figure 19**). Therefore, cortactin might be playing an important role in BM colonization by T-ALL cells. However, these experiments still need to be repeated with normal cortactin^{low} T cells to corroborate that they colonize BM spheroids less efficiently.

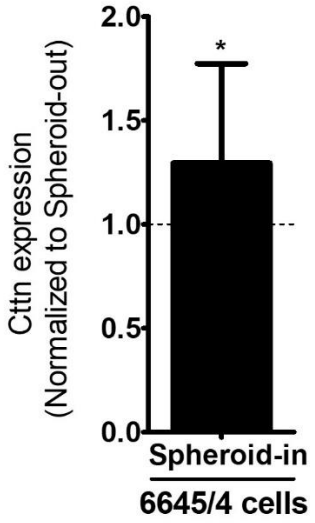

Figure 19. Expression of cortactin in 6645/4 cells co-cultured with OP9-GFP spheroids. Co-cultures were incubated for 24 hours. Then, spheroids were recovered, washed and disaggregated to obtain a single cell suspension. CD45$^+$Hoechst33342$^+$ cells inside the spheroids (in) were analyzed for cortactin expression and normalized to cortactin levels in cells outside the spheroids (set to 1, dotted line). Data are represented as fold MFI increase ± SD. Paired Student's t-test was performed to determine statistical significance. n=17. *p<0.05.

7. Discussion

Cortactin has recently emerged as an unfavorable prognosis marker in several types of solid cancers[143,144]. Surprisingly, cortactin has also been detected in leukemias such as B-CLL [136] and preB-ALL[142], despite being considered absent in normal lymphocytes. In this work, we characterized and evaluated the murine T-ALL cell line 6645/4, in which we detected a higher expression of cortactin when compared to normal T cells purified from spleen. In addition, high expression of cortactin correlated with increased transmigration capabilities *in vitro* as shown by transendothelial migration and spheroid co-culture assays.

The 6645/4 cell line was obtained from double transgenic mice expressing the SCL and LMO1 oncogenes which spontaneously developed T-ALL. In the first characterization performed by Chervinsky and colleagues, 6645/4 cells had low levels of CD3 and CD8, but high levels of CD4[138]. By contrast, our characterization revealed a high expression of CD3 and a low expression of CD8 (**Figure 12**). Moreover, CD4 was absent. In addition, we found that expression of the TCR signaling molecule CD3 in 6645/4 cells was found to be three times higher than in normal T cells (**Figure 13**). Therefore, we speculate that 6645/4 cells might possess a constitutively activated TCR signaling, since high expression of CD3 correlates with ZAP-70 kinase overexpression reported in T-ALL cells[103]. Thus, TCR signaling may endow 6645/4 cells with an activated T-cell phenotype leading to the activation of integrins[145], a prerequisite for transendothelial migration of T cells that could reinforce the infiltrative potential.

On the other hand, by analyzing CD44 and CD25 expression, we found that 6645/4 cells were in DN3 ($CD44^{-}CD25^{+}$) stage (**Figure 11**), in contrast to the reported DN2 ($CD44^{+}CD25^{+}$) stage of maturity by Chervinsky and colleagues, thus indicating a change in phenotype in this cell line over time. Such changes may be caused by genetic events such as translocations, since it has been observed that most cell lines had become aneuploidic[138], which is an effective mechanism to generate phenotypic variation[146], resulting from deregulation of transcriptome of cancer cells, due to gross number of genomic copy changes[147]. As reported in other cell lines

generated in the same study, two cell lines even lost the expression of both transgenes SCL and LMO1, while nonetheless remaining their tumorigenic capabilities[138]. Evaluating expression of these oncogenes, we found that 6645/4 cells maintained the expression of LMO1, whereas SCL expression was undetectable at mRNA level (**Figure 10**), suggesting that this cell line may have undergone additional mutations since the original report by Chervinsky and colleagues.

Among the many molecules overexpressed in leukemias, cortactin has recently been proposed as a poor prognostic factor in B-CLL and preB-ALL. Cortactin is an ABP with an important role in cytoskeletal rearrangements that are essential for cell motility in virtually all cell types. Recently, cortactin expression in B-CLL was also related to poor prognosis markers in these patients such as high expression of CD38 and ZAP-70[136]; whereas in preB-ALL, cortactin expression was related to bone marrow relapse and extramedullary infiltration[142]. In T-ALL cells from mice, cortactin expression was found to be driven by calcineurin, a calcium-dependent serin-threonin phosphatase previously demonstrated to be also overexpressed in T-ALL[108,109]. In addition, cortactin plays an important role in trafficking of the CXCL12 receptor CXCR4 to the cell membrane in murine T-ALL cells[101] CXCR4 membrane expression was dependent on cortactin levels, as cortactin-KD T-ALL cells showed diminished surface CXCR4 levels. Furthermore, cortactin-KD T-ALL cells had diminished chemotaxis towards a CXCL12 gradient suggesting a possible mechanism by which cortactin promotes CXCR4 signaling and thus T-ALL cell migration[101]. Analyzing the expression of cortactin and CXCR4 in 6645/4 cells, we observed a five-fold increase of cortactin and a 20-fold increase of CXCR4 in 6645/4 cells compared to normal T cells under basal conditions (**Figure 13**). Additionally, by evaluating the expression of cortactin in the populations that were able to transmigrate, we found higher levels of cortactin expression in the fraction of transmigrated 6645/4 (2.5% of transmigration) and normal T cells (1% of transmigration) (**Figure 16; Figure 18**). Importantly, cortactin expression in transmigrated T cells never even reached the level of non-transmigrated 6645/4 cells. Thus, we speculated that a cortactin-rich population within the 6645/4 cells

exists that has increased transmigration abilities. Indeed, we found a cortactin^{high} population in 6645/4 cell culture under basal conditions that correlated with bigger cell size (**Figure 19**). However, currently there is no functional relevance reported for bigger size, higher levels of cortactin and TEM in leukemic cells. Although more experiments are required to support this idea, our data support the importance of cortactin for TEM of these cells, as 6645/4 cells that expressed more cortactin had higher transmigration rates (**Figure 16; Figure 18**).

Cortactin overexpression in solid tumors commonly is a consequence of amplification of the 11q13 region, in which the cortactin-encoding EMS1 gene is located[135]. Nevertheless, it is currently unknown whether overexpression of cortactin in T-ALL cells can be attributed to gene amplification or, as suggested by Passaro et al., to a calcineurin-related pathway, since calcineurin-deficient T-ALL cells showed diminished levels of cortactin expression. However, further studies with exogenous expression of calcineurin need to be performed in order to confirm that cortactin overexpression in T-ALL cells is mediated by calcineurin.

Different cortactin variants have been reported to be expressed in B-CLL: B cells from B-CLL patients expressed both the wt- and the 70 kDa SV1-cortactin variant [136]; whereas preB-ALL cell lines and preB cells from B-ALL patients exclusively expressed the 60 kDa SV2-cortactin variant[142]. Hitherto, three cortactin variants have been reported: the 80 kDa full-length cortactin (wt-cortactin), the 70 kDa SV1-cortactin lacking repeat 6 (exon 11) and the 60 kDa SV2-cortactin lacking repeat 5 and 6 (exon 10 and 11) (**Figure 9**)[129]. Data from our work group revealed high levels of cortactin expression in preB-ALL leukemic cells leading to an improved ability to transmigrate, in spite of expressing only the 60 KDa SV2-cortactin form[142]. Although the wt- and SV1-cortactin forms have higher affinities for F-actin, the SV2-cortactin still contains the fourth repeat, which is essential for actin binding, and thus induction of Arp2/3-mediated actin polymerization[116]. When we analyzed the expression of cortactin in 6645/4 cells and normal T cells by western blot (**Figure 14**), we found that both cell types expressed only the 80 kDa wt-cortactin isoform, although the levels were much higher in leukemic T cells. Hitherto,

cortactin expression in normal mouse T cells has not been reported, making this an interesting new finding. The functional relevance of different expression of cortactin isoforms is currently unclear. However, as mentioned above, the different abilities of the isoforms to bind and cross-link F-actin and to activate the Arp2/3 complex[116,129], may explain the different needs of the different cells for different cortactin isoforms. Thus, overexpression of the 80 kDa wt-cortactin variant cortactin may give further insight into understanding the high infiltration rates of T-ALL among lymphoblastic leukemias.

On the other hand, we found by flow cytometry that expression of the cortactin homologue HS1 was only increased 1.2-fold in 6645/4 cells compared to normal T cells, similarly to what was reported for B-CLL, where expression of HS1 in B-CLL cells was increased 1.38-fold compared to normal B-cells[148]. Despite the small increase, overxpression of HS1 in B-CLL was related to a poor prognosis[136]. Moreover, our group found an overexpression of HS1 in the preB-ALL cell lines REH and RS4 as well as in pediatric B-ALL patients[142]. However, the relation to risk factors has not yet been explored in this type of leukemia.

In vitro transmigration assays using 6645/4 leukemic T cells showed that only 2.5% of total cells transmigrated through bEnd.5 monolayers towards a CXCL12 gradient. However, only 1% of normal T cells transmigrated under the same conditions showing that leukemic T cells had a significant transmigratory advantage over normal T cells (**Figure 17**). Importantly, VLA-4 expression as well as CXCR4 expression in 6645/4 leukemic cells was higher compared to normal T cells that may also contribute to the transmigratory advantage (**Figure 13**). Integrins must undergo conformational rearrangement to achieve the high affinity state in response to chemokines such as CXCL12. Thus, high CXCR4 expression might increase integrin activation, thus promoting cell adhesion and subsequent transmigration. The CXCR4 ligand CXCL12 is constantly produced by bone marrow endothelial cells to support migration, proliferation and differentiation of HSC[149]. CXCL12 production in the BM is critical for lymphopoiesis under normal conditions. However, T-ALL cells overexpressing CXCR4 established themselves

in CXCL12-rich BM niches[102,150]. Furthermore, Passaro and colleagues demonstrated that conditional deletion of CXCR4 in T-ALL mice reduced the infiltration to BM, diminished the proliferation rates and rendered T-ALL cells more susceptible to apoptosis.

In addition to increased TEM, we found that only 6645/4 cells expressing high levels of cortactin were able to colonize *in vitro* BM spheroids. However, what we would like to call a comparison with cortactin^{low} normal T cells remains to be done in order to corroborate a functional association between BM colonization and high cortactin expression. It appears that small fractions of leukemic T cells that are endowed with higher migration abilities (due to high CXCR4 and cortactin expression) might reach the BM or organs such as brain and testis more easily, thus evading chemotherapy and giving rise to treatment failure and relapse. These cells might then act as what we would like to call relapse-initiating cells (RICs). However, more thorough characterization of this cortactin-high and CXCR4-high 6645/4 cell population; and xenotransplant assays with these cells have to be done in order to better understand the aggressiveness of this cell line. Furthermore, to unequivocally prove the requirement of these proteins in these processes, we are currently in the process of establishing 6645/4 cell lines depleted for either cortactin or CXCR4.

Taken together, the results obtained in this work suggest an important role of cortactin in leukemic T cell infiltration as its expression correlated with increased transmigration abilities through endothelial bEnd.5 monolayers. In addition, cortactin might be a suitable pharmacological target to prevent T-ALL relapse by reducing transendothelial migration, organ infiltration, and, as reported by others[101], by reducing the expression of CXCR4 on the surface of leukemic cells.

8. Conclusion

The murine T-ALL cell line 6645/4 expresses the proteins needed to accomplish transendothelial migration. Moreover, these cells express high levels of the 80 KDa wt-cortactin isoform and CXCR4, thus endowing these leukemic T cells with a transmigratory advantage. Cortactin overexpression might be associated with T-ALL aggressiveness and the high rate of infiltration.

9. Perspectives

1. To perform transplants of leukemic 6645/4 T cells into NSG recipient mice to analyze the infiltrative potential of these cells in vivo.

2. To generate a cortactin-KD in mouse and human T-ALL cell lines to evaluate the role of cortactin in transmigration and invasion.

3. To analyze the expression and functional relevance of cortactin in patient-derived samples of T-ALL and ETP-ALL.

10. References

1. Ferlay, J. *et al.* Cancer incidence and mortality worldwide: Sources, methods and major patterns in GLOBOCAN 2012. *Int. J. Cancer* **136,** E359–E386 (2015).

2. Pérez-Saldivar, M. L. *et al.* Childhood acute leukemias are frequent in Mexico City: Descriptive epidemiology. *BMC Cancer* **11,** 355 (2011).

3. Deng, X. *et al.* Wnt 5a and CCL25 promote adult T-cell acute lymphoblastic leukemia cell migration, invasion and metastasis. *Oncotarget* **8,** 39033–39047 (2017).

4. Coustan-Smith, E. *et al.* Early T-Cell Precursor Leukemia: A Subtype of Very High-Risk Acute Lymphoblastic Leukemia Identified in Two Independant Cohorts. *Lancet The* **10,** 147–156 (2010).

5. Goldberg, J. M. *et al.* Childhood T-cell acute lymphoblastic leukemia: The Dana-Farber Cancer Institute Acute Lymphoblastic Leukemia Consortium experience. *J. Clin. Oncol.* **21,** 3616–3622 (2003).

6. Attarbaschi, A. *et al.* Mediastinal mass in childhood T-cell acute lymphoblastic leukemia: Significance and therapy response. *Med. Pediatr. Oncol.* **39,** 558–565 (2002).

7. Cook, L. B. *et al.* The role of HTLV-1 clonality, proviral structure, and genomic integration site in adult T-cell leukemia/lymphoma. *Blood* (2014). doi:10.1182/blood-2014-02-553602

8. Juncà, J., Botín, T., Vila, J., Navarro, J. T. & Millá, F. Adult T-cell leukemia/lymphoma with an unusual CD1a positive phenotype. *Cytom. Part B - Clin. Cytom.* **86,** 292–296 (2014).

9. Díaz Torres, H. M. *et al.* [Human T-cell lymphotropic virus type I infection in patients with lymphoproliferative disorders at two sentinel sites in Cuba]. *Rev. Panam. Salud Publica* **27,** 17–22 (2010).

10. Pérez-Saldivar, M. L. *et al.* Parental Exposure to Workplace Carcinogens and the Risk of Development of Acute Leukemia in Infants. Case-Control Study. *Arch. Med. Res.* **47,** 684–693 (2016).

11. Esparza-López, J., Escobar-Arriaga, E., Soto-Germes, S. & De Jesus Ibarra-Sanchez, M. Breast cancer intra-tumor heterogeneity: One tumor, different entities. *Rev. Investig. Clin.* **69,** 66–76 (2017).

12. Greaves, M. & Maley, C. C. Clonal evolution in cancer. *Nature* **481,** 306–313 (2012).

13. Meacham, C. E. & Morrison, S. J. Tumour heterogeneity and cancer cell plasticity. *Nature* **501,** 328–337 (2013).

14. Enciso, J., Mendoza, L. & Pelayo, R. Normal vs. Malignant hematopoiesis: The complexity of acute leukemia through systems biology. *Front. Genet.* **6,** 1–5 (2015).

15. Tremblay, M., Tremblay, C. S., Herblot, S., Tremblay, S. & Aplan, P. D. Modeling T-cell acute lymphoblastic leukemia induced by the SCL Modeling T-cell acute lymphoblastic leukemia induced by the SCL and LMO1 oncogenes. *Genes Dev.* 1093–1105 (2010). doi:10.1101/gad.1897910

16. Vilchis-Ordo, A., Dorantes-Acosta, E., Vadillo, E., López-Martínez, B. & Pelayo, R. Early hematopoietic differentiation in acute lymphoblastic leukemia: The interplay between leukemia-initiating cells and abnormal bone marrow microenvironment. in *Etiology of Acute Leukemias in Children* (2016). doi:10.1007/978-3-319-05798-9_9

17. Bonnet, D. & Dick, J. E. Human acute myeloid leukemia is organized as a hierarchy that originates from a primitive hematopoietic cell. *Nat. Med.* (1997). doi:10.1038/nm0797-730

18. Lapidot, T. *et al.* A cell initiating human acute myeloid leukaemia after transplantation into SCID mice. *Nature* (1994). doi:10.1038/367645a0

19. Wang, J. C. *et al.* High level engraftment of NOD/SCID mice by primitive normal and leukemic hematopoietic cells from patients with chronic myeloid leukemia in chronic phase. *Blood* (1998).

20. Al-Hajj, M., Wicha, M. S., Benito-Hernandez, A., Morrison, S. J. & Clarke, M. F. Prospective identification of tumorigenic breast cancer cells. *Proc. Natl. Acad. Sci.* (2003). doi:10.1073/pnas.0530291100

21. Singh, S. K. *et al.* Identification of human brain tumour initiating cells. *Nature* (2004).

doi:10.1038/nature03128

22. Dalerba, P. *et al.* Phenotypic characterization of human colorectal cancer stem cells. *Proc. Natl. Acad. Sci. U. S. A.* (2007). doi:10.1073/pnas.0703478104

23. O'Brien, C. A., Pollett, A., Gallinger, S. & Dick, J. E. A human colon cancer cell capable of initiating tumour growth in immunodeficient mice. *Nature* (2007). doi:10.1038/nature05372

24. Ricci-Vitiani, L. *et al.* Identification and expansion of human colon-cancer-initiating cells. *Nature* (2007). doi:10.1038/nature05384

25. Li, C. *et al.* Identification of pancreatic cancer stem cells. *Cancer Res.* (2007). doi:10.1158/0008-5472.CAN-06-2030

26. Curley, M. D. *et al.* CD133 expression defines a tumor initiating cell population in primary human ovarian cancer. *Stem Cells* (2009). doi:10.1002/stem.236

27. Zhang, S. *et al.* Identification and characterization of ovarian cancer-initiating cells from primary human tumors. *Cancer Res.* (2008). doi:10.1158/0008-5472.CAN-08-0364

28. Stewart, J. M. *et al.* Phenotypic heterogeneity and instability of human ovarian tumor-initiating cells. *Proc. Natl. Acad. Sci. U. S. A.* (2011). doi:10.1073/pnas.1005529108

29. Nowell, P. C. The clonal evolution of tumor cell populations. *Science* (1976). doi:10.1126/science.959840

30. Burrell, R. A., McGranahan, N., Bartek, J. & Swanton, C. The causes and consequences of genetic heterogeneity in cancer evolution. *Nature* (2013). doi:10.1038/nature12625

31. Geyer, F. C. *et al.* Molecular analysis reveals a genetic basis for the phenotypic diversity of metaplastic breast carcinomas. *J. Pathol.* (2010). doi:10.1002/path.2675

32. Swaminathan, S. *et al.* Mechanisms of clonal evolution in childhood acute lymphoblastic leukemia. *Nat. Immunol.* **16,** 766–774 (2015).

33. Balandrï¿½n, J. C. *et al.* Pro-inflammatory-related loss of CXCL12 niche promotes

acute lymphoblastic leukemic progression at the expense of normal lymphopoiesis. *Front. Immunol.* **7,** 1–14 (2017).

34. le Viseur, C. *et al.* In Childhood Acute Lymphoblastic Leukemia, Blasts at Different Stages of Immunophenotypic Maturation Have Stem Cell Properties. *Cancer Cell* **14,** 47–58 (2008).

35. Rehe, K. *et al.* Acute B lymphoblastic leukaemia-propagating cells are present at high frequency in diverse lymphoblast populations. *EMBO Mol. Med.* **5,** 38–51 (2013).

36. Reya, T., Morrison, S. J., Clarke, M. F. & Weissman, I. L. Stem cells, cancer, and cancer stem cells. *Nature* (2001). doi:10.1038/35102167

37. Pear, W. S. Exclusive development of T cell neoplasms in mice transplanted with bone marrow expressing activated Notch alleles. *J. Exp. Med.* **183,** 2283–2291 (1996).

38. Girardi, T., Vicente, C., Cools, J. & Keersmaecker, K. De. Europe PMC Funders Group The genetics and molecular biology of T-ALL. **129,** 1113–1123 (2017).

39. Van Vlierberghe, P., Ferrando, A., Vlierberghe, P. Van & Ferrando, A. The molecular es basis of T cell acute lymphoblastic leukemia. *J. Clin. Invest.* (2012). doi:10.1172/JCI61269.3398

40. Trinquand, A. *et al.* Toward a NOTCH1/FBXW7/RAS/PTEN-based oncogenetic risk classification of adult T-Cell acute lymphoblastic leukemia: A group for research in adult acute lymphoblastic leukemia study. *J. Clin. Oncol.* (2013). doi:10.1200/JCO.2012.48.5292

41. Belver, L. & Ferrando, A. The genetics and mechanisms of T cell acute lymphoblastic leukaemia. *Nat. Rev. Cancer* **16,** 494–507 (2016).

42. Padi, S. K. R. *et al.* Targeting the PIM protein kinases for the treatment of a T-cell acute lymphoblastic leukemia subset. *Oncotarget* **8,** 30199–30216 (2017).

43. Pieters, R. & Carroll, W. L. Biology and Treatment of Acute Lymphoblastic Leukemia. *Hematology/Oncology Clinics of North America* (2010). doi:10.1016/j.hoc.2009.11.014

44. Hahn, T. *et al.* The Role of Cytotoxic Therapy with Hematopoietic Stem Cell Transplantation in the Therapy of Acute Lymphoblastic Leukemia in Children: An Evidence-Based Review. *Biol. Blood Marrow Transplant.* (2005). doi:10.1016/j.bbmt.2005.08.035

45. Locatelli, F., Schrappe, M., Bernardo, M. E. & Rutella, S. How i treat relapsed childhood acute lymphoblastic leukemia. *Blood* (2012). doi:10.1182/blood-2012-02-265884

46. Weng, A. P. *et al.* Activating mutations of NOTCH1 in human T cell acute lymphoblastic leukemia. *Science* (2004). doi:10.1126/science.1102160

47. Wallberg, A. E., Pedersen, K., Lendahl, U. & Roeder, R. G. p300 and PCAF act cooperatively to mediate transcriptional activation from chromatin templates by notch intracellular domains in vitro. *Mol. Cell. Biol.* (2002). doi:10.1128/MCB.22.22.7812-7819.2002

48. Fryer, C. J., Lamar, E., Turbachova, I., Kintner, C. & Jones, K. A. Mastermind mediates chromatin-specific transcription and turnover of the notch enhancer complex. *Genes Dev.* (2002). doi:10.1101/gad.991602

49. Degryse, S. & Cools, J. JAK kinase inhibitors for the treatment of acute lymphoblastic leukemia. *J. Hematol. Oncol.* (2014). doi:10.1186/s13045-015-0192-7

50. Subramaniam, P. S. *et al.* Targeting Nonclassical Oncogenes for Therapy in T-ALL. *Cancer Cell* (2012). doi:10.1016/j.ccr.2012.02.029

51. Fala, F. *et al.* Proapoptotic activity and chemosensitizing effect of the novel Akt inhibitor (2S)-1-(1H-Indol-3-yl)-3-[5-(3-methyl-2H-indazol-5-yl)pyridin-3-yl]oxyprop an2-amine (A443654) in T-cell acute lymphoblastic leukemia. *Mol Pharmacol* (2008). doi:mol.108.047639 [pii]\n10.1124/mol.108.047639

52. Chiarini, F. *et al.* The novel Akt inhibitor, perifosine, induces caspase-dependent apoptosis and downregulates P-glycoprotein expression in multidrug-resistant human T-acute leukemia cells by a JNK-dependent mechanism. *Leukemia* (2008). doi:10.1038/leu.2008.79

53. Evangelisti, C. *et al.* Targeted inhibition of mTORC1 and mTORC2 by active-site

mTOR inhibitors has cytotoxic effects in T-cell acute lymphoblastic leukemia. *Leukemia* (2011). doi:10.1038/leu.2011.20

54. Martelli, A. M. *et al.* Targeting the translational apparatus to improve leukemia therapy: Roles of the PI3K/PTEN/Akt/mTOR pathway. *Leukemia* (2011). doi:10.1038/leu.2011.46

55. Litzow, M. Rh. I. T. H. I. treat T. acute lymphoblastic leukemia in adults & Ferrando, A. A. How I treat T-cell acute lymphoblastic leukemia in adults. *Blood* **126,** 833–842 (2015).

56. Coleman, R. E. Glucocorticoids in cancer therapy. *Biotherapy* (1992). doi:10.1007/BF02171708

57. Peirs, S. *et al.* ABT-199 mediated inhibition of BCL-2 as a novel therapeutic strategy in T-cell acute lymphoblastic leukemia. *Blood* (2014). doi:10.1182/blood-2014-05-574566

58. Ni Chonghaile, T. *et al.* Maturation stage of T-cell acute lymphoblastic leukemia determines BCL-2 versus BCL-XL dependence and sensitivity to ABT-199. *Cancer Discov.* (2014). doi:10.1158/2159-8290.CD-14-0353

59. Lüpertz, R., Wätjen, W., Kahl, R. & Chovolou, Y. Dose- and time-dependent effects of doxorubicin on cytotoxicity, cell cycle and apoptotic cell death in human colon cancer cells. *Toxicology* (2010). doi:10.1016/j.tox.2010.03.012

60. Verma, N., Kumar, K., Kaur, G. & Anand, S. L-asparaginase: A promising chemotherapeutic agent. *Critical Reviews in Biotechnology* (2007). doi:10.1080/07388550601173926

61. Egler, R., Ahuja, S. & Matloub, Y. L-asparaginase in the treatment of patients with acute lymphoblastic leukemia. *J. Pharmacol. Pharmacother.* (2016). doi:10.4103/0976-500X.184769

62. Pui, C. H. & Howard, S. C. Current management and challenges of malignant disease in the CNS in paediatric leukaemia. *Lancet Oncol.* **9,** 257–268 (2008).

63. Çekiç, O., Biberoglu, E. & Esen, F. Peripapillary retinal leukemic infiltration associated with papilledema in a T-ALL patient without cranial or optic nerve

involvement. *Tumori* (2016). doi:10.5301/tj.5000490

64. Kay, H. E. M. TESTICULAR INFILTRATION IN ACUTE LYMPHOBLASTIC LEUKAEMIA. *Br. J. Haematol.* (1983). doi:10.1111/j.1365-2141.1983.tb07305.x

65. Atarashi, K., Hirata, T., Matsumoto, M., Kanemitsu, N. & Miyasaka, M. Rolling of Th1 Cells via P-Selectin Glycoprotein Ligand-1 Stimulates LFA-1-Mediated Cell Binding to ICAM-1. *J. Immunol.* **174,** 1424–1432 (2005).

66. Schnoor, M., Alcaide, P., Voisin, M. B. & Van Buul, J. D. Crossing the Vascular Wall: Common and Unique Mechanisms Exploited by Different Leukocyte Subsets during Extravasation. *Mediators Inflamm.* **2015,** (2015).

67. Nourshargh, S., Hordijk, P. L. & Sixt, M. Breaching multiple barriers: Leukocyte motility through venular walls and the interstitium. *Nat. Rev. Mol. Cell Biol.* **11,** 366–378 (2010).

68. Timmerman, I., Daniel, A. E., Kroon, J. & Van Buul, J. D. Leukocytes Crossing the Endothelium: A Matter of Communication. *Int. Rev. Cell Mol. Biol.* **322,** 281–329 (2016).

69. Woodfin, A. *et al.* The junctional adhesion molecule JAM-C regulates polarized transendothelial migration of neutrophils in vivo. *Nat. Immunol.* (2011). doi:10.1038/ni.2062

70. Schaefer, A. *et al.* Actin-binding proteins differentially regulate endothelial cell stiffness, ICAM-1 function and neutrophil transmigration. *J. Cell Sci.* **127,** 4985–4985 (2014).

71. Martinelli, R. *et al.* Probing the biomechanical contribution of the endothelium to lymphocyte migration: diapedesis by the path of least resistance. *J. Cell Sci.* **127,** 3720–3734 (2014).

72. Sigmundsdottir, H. & Butcher, E. C. Environmental cues, dendritic cells and the programming of tissue-selective lymphocyte trafficking. *Nat. Immunol.* **9,** 981–987 (2008).

73. Takeda, A., Sasaki, N. & Miyasaka, M. The molecular cues regulating immune cell trafficking. *Proc. Jpn. Acad. Ser. B. Phys. Biol. Sci.* **93,** 183–195 (2017).

74. Lee, M. *et al.* Transcriptional programs of lymphoid tissue capillary and high endothelium reveal control mechanisms for lymphocyte homing. *Nat. Immunol.* (2014). doi:10.1038/ni.2983

75. Marsal, J. & Agace, W. W. Targeting T-cell migration in inflammatory bowel disease. *Journal of Internal Medicine* (2012). doi:10.1111/j.1365-2796.2012.02588.x

76. Campbell, J. J. *et al.* Chemokines and the arrest of lymphocytes rolling under flow conditions. *Science (80-.).* (1998). doi:10.1126/science.279.5349.381

77. Manes, T. D. & Pober, J. S. Antigen Presentation by Human Microvascular Endothelial Cells Triggers ICAM-1-Dependent Transendothelial Protrusion by, and Fractalkine-Dependent Transendothelial Migration of, Effector Memory CD4+ T Cells. *J. Immunol.* **180,** 8386–8392 (2008).

78. Engelhardt, B. Molecular mechanisms involved in T cell migration across the blood-brain barrier. *J. Neural Transm.* **113,** 477–485 (2006).

79. Vestweber, D. How leukocytes cross the vascular endothelium. *Nat. Rev. Immunol.* **15,** 692–704 (2015).

80. Atarashi, K., Hirata, T., Matsumoto, M., Kanemitsu, N. & Miyasaka, M. Rolling of Th1 Cells via P-Selectin Glycoprotein Ligand-1 Stimulates LFA-1-Mediated Cell Binding to ICAM-1. *J. Immunol.* (2005). doi:10.4049/jimmunol.174.3.1424

81. Madri, J. & Graesser, D. Cell migration in the immune system: the evolving inter-related roles of adhesion molecules and proteinases. *Dev. Immunol.* **7,** 103–116 (2000).

82. Cook-Mills, J. M. Active participation of endothelial cells in inflammation. *J. Leukoc. Biol.* (2004). doi:10.1189/jlb.0904554

83. Springer, T. A. & Dustin, M. L. Integrin inside-out signaling and the immunological synapse. *Current Opinion in Cell Biology* (2012). doi:10.1016/j.ceb.2011.10.004

84. Laffon, A. *et al.* Upregulated expression and function of VLA-4 fibronectin receptors on human activated T cells in rheumatoid arthritis. *J Clin Invest* **88,** 546–552 (1991).

85. Bönig, H. & Kim, Y. Targeted Therapy of Acute Myeloid Leukemia. 637–654 (2015).

doi:10.1007/978-1-4939-1393-0

86. Chigaev, A., Wu, Y., Williams, D. B., Smagley, Y. & Sklar, L. A. Discovery of Very Late Antigen-4 (VLA-4, α4β 1 integrin) allosteric antagonists. *J. Biol. Chem.* **286,** 5455–5463 (2011).

87. Hyun, Y.-M., Chung, H.-L., McGrath, J. L., Waugh, R. E. & Kim, M. Activated Integrin VLA-4 Localizes to the Lamellipodia and Mediates T Cell Migration on VCAM-1. *J. Immunol.* **183,** 359–369 (2009).

88. Van Rijssel, J. *et al.* The Rho-GEF Trio regulates a novel pro-inflammatory pathway through the transcription factor Ets2. *Biol. Open* (2013). doi:10.1242/bio.20134382

89. van Buul JD, H. P. L. Signaling in leukocyte transendothelial migration. *Arter. Thromb Vasc Biol* **24,** 824–833 (2004).

90. Förster, R. *et al.* CCR7 coordinates the primary immune response by establishing functional microenvironments in secondary lymphoid organs. *Cell* (1999). doi:10.1016/S0092-8674(00)80059-8

91. Nakano, H. *et al.* Genetic defect in T lymphocyte-specific homing into peripheral lymph nodes. *Eur. J. Immunol.* (1997). doi:10.1002/eji.1830270132

92. Bajénoff, M. *et al.* Stromal Cell Networks Regulate Lymphocyte Entry, Migration, and Territoriality in Lymph Nodes. *Immunity* (2006). doi:10.1016/j.immuni.2006.10.011

93. Proebstl, D. *et al.* Pericytes support neutrophil subendothelial cell crawling and breaching of venular walls in vivo. *J. Exp. Med.* (2012). doi:10.1084/jem.20111622

94. Soehnlein, O., Lindbom, L. & Weber, C. Mechanisms underlying neutrophil-mediated monocyte recruitment. *Blood* (2009). doi:10.1182/blood-2009-06-221630

95. Mydel, P. *et al.* Neutrophil elastase cleaves laminin-332 (laminin-5) generating peptides that are chemotactic for neutrophils. *J. Biol. Chem.* (2008). doi:10.1074/jbc.M706239200

96. Muller, W. A. Mechanisms of Leukocyte Transendothelial Migration. *Annu. Rev. Pathol. Mech. Dis.* (2011). doi:10.1146/annurev-pathol-011110-130224

97. Iijima, N. & Iwasaki, A. Tissue instruction for migration and retention of T<inf>RM</inf> cells. *Trends in Immunology* (2015). doi:10.1016/j.it.2015.07.002

98. Jost, T. R. *et al.* Role of CXCR4-mediated bone marrow colonization in CNS infiltration by T cell acute lymphoblastic leukemia. *J. Leukoc. Biol.* **99,** 1077–1087 (2016).

99. Hashiguchi, T. *et al.* Adult T-cell leukemia (ATL) cells which express neural cell adhesion molecule (NCAM) and infiltrate into the central nervous system. *Intern. Med.* **41,** 34–38 (2002).

100. Ishikawa, T. *et al.* E-selectin and vascular cell adhesion molecule-1 mediate adult T-cell leukemia cell adhesion to endothelial cells. *Blood* **82,** 1590–1598 (1993).

101. Passaro, D. *et al.* CXCR4 Is Required for Leukemia-Initiating Cell Activity in T Cell Acute Lymphoblastic Leukemia. *Cancer Cell* **27,** 769–779 (2015).

102. Pitt, L. A. *et al.* CXCL12-Producing Vascular Endothelial Niches Control Acute T Cell Leukemia Maintenance. *Cancer Cell* **27,** 755–768 (2015).

103. Alsadeq, A. *et al.* The role of ZAP70 kinase in acute lymphoblastic leukemia infiltration into the central nervous system. *Haematologica* **102,** 346–355 (2017).

104. Melo, R. D. C. C. *et al.* CXCR7 is highly expressed in acute lymphoblastic leukemia and potentiates CXCR4 response to CXCL12. *PLoS One* **9,** 1–12 (2014).

105. Buonamici, S. *et al.* CCR7 signalling as an essential regulator of CNS infiltration in T-cell leukaemia. *Nature* **459,** 1000–1004 (2009).

106. Wang, H. *et al.* ZAP-70: an essential kinase in T-cell signaling. *Cold Spring Harbor perspectives in biology* (2010). doi:10.1101/cshperspect.a002279

107. de Bock, C. E. & Cools, J. T-ALL: Home Is where the CXCL12 Is. *Cancer Cell* **27,** 745–746 (2015).

108. Medyouf, H. *et al.* Targeting calcineurin activation as a therapeutic strategy for T-cell acute lymphoblastic leukemia. *Nat. Med.* **13,** 736–741 (2007).

109. Gachet, S. *et al.* Leukemia-initiating cell activity requires calcineurin in T-cell acute lymphoblastic leukemia. *Leukemia* **27,** 2289–2300 (2013).

110. Wu, H., Reynolds, A. B., Kanner, S. B., Vines, R. R. & Parsons, J. T. Identification and characterization of a novel cytoskeleton-associated pp60src substrate. *Mol. Cell. Biol.* (1991). doi:10.1128/MCB.11.10.5113

111. Schnoor, M., Stradal, T. E. & Rottner, K. Cortactin: Cell Functions of A Multifaceted Actin-Binding Protein. *Trends in Cell Biology* (2017). doi:10.1016/j.tcb.2017.10.009

112. Weed, S. A. & Parsons, J. T. Cortactin: Coupling membrane dynamics to cortical actin assembly. *Oncogene* (2001). doi:10.1038/sj.onc.1204783

113. Shvetsov, A., Berkane, E., Chereau, D., Dominguez, R. & Reisler, E. The actin-binding domain of cortactin is dynamic and unstructured and affects lateral and longitudinal contacts in F-actin. *Cell Motil. Cytoskeleton* (2009). doi:10.1002/cm.20328

114. Buday, L. & Downward, J. Roles of cortactin in tumor pathogenesis. *Biochimica et Biophysica Acta - Reviews on Cancer* (2007). doi:10.1016/j.bbcan.2006.12.002

115. Martinez-Quiles, N. Emerging roles of haematopoietic lineage cell-specific protein 1 in the immune system. *OA Immunol.* **1,** 1–7 (2003).

116. Weed, S. A. *et al.* Cortactin localization to sites of actin assembly in lamellipodia requires interactions with F-actin and the Arp2/3 complex. *J. Cell Biol.* (2000). doi:10.1083/jcb.151.1.29

117. Lua, B. L. & Low, B. C. Cortactin phosphorylation as a switch for actin cytoskeletal network and cell dynamics control. *FEBS Letters* (2005). doi:10.1016/j.febslet.2004.12.055

118. Yin, M., Ma, W. & An, L. Cortactin in cancer cell migration and invasion. *Oncotarget* **8,** 88232–88243 (2017).

119. Weed, S. a, Du, Y. & Parsons, J. T. Translocation of cortactin to the cell periphery is mediated by the small GTPase Rac1. *J. Cell Sci.* (1998).

120. Burkhardt, J. K., Carrizosa, E. & Shaffer, M. H. The Actin Cytoskeleton in T Cell Activation. *Annu. Rev. Immunol.* (2008). doi:10.1146/annurev.immunol.26.021607.090347

121. MacGrath, S. M. & Koleske, A. J. Cortactin in cell migration and cancer at a glance. *J. Cell Sci.* **125,** 1621–1626 (2012).

122. Martinez-Quiles, N., Ho, H.-Y. H., Kirschner, M. W., Ramesh, N. & Geha, R. S. Erk/Src Phosphorylation of Cortactin Acts as a Switch On-Switch Off Mechanism That Controls Its Ability To Activate N-WASP. *Mol. Cell. Biol.* (2004). doi:10.1128/MCB.24.12.5269-5280.2004

123. Kowalski, J. R. *et al.* Cortactin regulates cell migration through activation of N-WASP. *J Cell Sci* (2005). doi:10.1242/jcs.01586

124. Kruchten, A. E., Krueger, E. W., Wang, Y. & McNiven, M. A. Distinct phospho-forms of cortactin differentially regulate actin polymerization and focal adhesions. *Am. J. Physiol. Physiol.* (2008). doi:10.1152/ajpcell.00238.2008

125. Zhang, X. *et al.* HDAC6 Modulates Cell Motility by Altering the Acetylation Level of Cortactin. *Mol. Cell* (2007). doi:10.1016/j.molcel.2007.05.033

126. Zhang, Y. *et al.* Deacetylation of cortactin by SIRT1 promotes cell migration. *Oncogene* (2009). doi:10.1038/onc.2008.388

127. Rey, M., Irondelle, M., Waharte, F., Lizarraga, F. & Chavrier, P. HDAC6 is required for invadopodia activity and invasion by breast tumor cells. *Eur. J. Cell Biol.* (2011). doi:10.1016/j.ejcb.2010.09.004

128. van Rossum, A. G. S. H., Schuuring-Scholtes, E., van Buuren-van Seggelen, V., Kluin, P. M. & Schuuring, E. Comparative genome analysis of cortactin and HS1: The significance of the F-actin binding repeat domain. *BMC Genomics* (2005). doi:10.1186/1471-2164-6-15

129. van Rossum, A. G. S. H. *et al.* Alternative Splicing of the Actin Binding Domain of Human Cortactin Affects Cell Migration. *J. Biol. Chem.* **278,** 45672–45679 (2003).

130. Yuan, B. Z., Zhou, X., Zimonjic, D. B., Durkin, M. E. & Popescu, N. C. Amplification and overexpression of the EMS 1 oncogene, a possible prognostic marker, in human hepatocellular carcinoma. *J. Mol. Diagnostics* (2003). doi:10.1016/S1525-1578(10)60451-5

131. Myllykangas, S., Böhling, T. & Knuutila, S. Specificity, selection and significance of

gene amplifications in cancer. *Seminars in Cancer Biology* (2007). doi:10.1016/j.semcancer.2006.10.005

132. Luo, M. L. *et al.* Amplification and overexpression of CTTN (EMS1) contribute to the metastasis of esophageal squamous cell carcinoma by promoting cell migration and anoikis resistance. *Cancer Res.* (2006). doi:10.1158/0008-5472.CAN-06-1484

133. Ni, Q. F. *et al.* Cortactin promotes colon cancer progression by regulating ERK pathway. *Int. J. Oncol.* (2015). doi:10.3892/ijo.2015.3072

134. Schuuring, E., Verhoeven, E., Mooi, W. J. & Michalides, R. J. Identification and cloning of two overexpressed genes, U21B31/PRAD1 and EMS1, within the amplified chromosome 11q13 region in human carcinomas. *Oncogene* (1992).

135. Lázár, V. *et al.* Characterization of candidate gene copy number alterations in the 11q13 region along with BRAF and NRAS mutations in human melanoma. *Mod. Pathol.* (2009). doi:10.1038/modpathol.2009.109

136. Gattazzo, C. *et al.* Cortactin, another player in the Lyn signaling pathway, is over-expressed and alternatively spliced in leukemic cells from patients with B-cell chronic lymphocytic leukemia. *Haematologica* **99,** 1069–1077 (2014).

137. Martini, V. *et al.* Cortactin, a Lyn substrate, is a checkpoint molecule at the intersection of BCR and CXCR4 signalling pathway in chronic lymphocytic leukaemia cells. *Br. J. Haematol.* **178,** 81–93 (2017).

138. Chervinsky, D. S., Lam, D. H., Zhao, X. F., Melman, M. P. & Aplan, P. D. Development and characterization of T cell leukemia cell lines established from SCL/LMO1 double transgenic mice. *Leuk. Off. J. Leuk. Soc. Am. Leuk. Res. Fund UK* **15,** 141–147 (2001).

139. Itoh, K. *et al.* Reproducible establishment of hemopoietic supportive stromal cell lines from murine bone marrow. *Experimental hematology* (1989).

140. McGuire, E. A., Rintoul, C. E., Sclar, G. M. & Korsmeyer, S. J. Thymic overexpression of Ttg-1 in transgenic mice results in T-cell acute lymphoblastic leukemia/lymphoma. *Mol. Cell. Biol.* (1992). doi:10.1128/MCB.12.9.4186

141. Durinck, K. *et al.* Novel biological insights in T-cell acute lymphoblastic leukemia.

Exp. Hematol. **43,** 625–639 (2015).

142. Velázquez, M. The role of cortactin in the transmigration of leukemic precursors in B-lineage acute lymphoblastic leukemia. (PhD Thesis, 2018).

143. Leong, H. S. *et al.* Invadopodia Are Required for Cancer Cell Extravasation and Are a Therapeutic Target for Metastasis. *Cell Rep.* (2014). doi:10.1016/j.celrep.2014.07.050

144. Yamaguchi, H. & Condeelis, J. Regulation of the actin cytoskeleton in cancer cell migration and invasion. *Biochimica et Biophysica Acta - Molecular Cell Research* (2007). doi:10.1016/j.bbamcr.2006.07.001

145. Gronholm, M. *et al.* TCR-Induced Activation of LFA-1 Involves Signaling through Tiam1. *J. Immunol.* (2011). doi:10.4049/jimmunol.1100704

146. Gordon, D. J., Resio, B. & Pellman, D. Causes and consequences of aneuploidy in cancer. *Nature Reviews Genetics* (2012). doi:10.1038/nrg3123

147. Ried, T. *et al.* The consequences of chromosomal aneuploidy on the transcriptome of cancer cells. *Biochimica et Biophysica Acta - Gene Regulatory Mechanisms* (2012). doi:10.1016/j.bbagrm.2012.02.020

148. Frezzato, F. *et al.* HS1, a lyn kinase substrate, is abnormally expressed in B-chronic lymphocytic leukemia and correlates with response to fludarabine-based regimen. *PLoS One* (2012). doi:10.1371/journal.pone.0039902

149. Sison, E. A. R. & Brown, P. The bone marrow microenvironment and leukemia: Biology and therapeutic targeting. *Expert Review of Hematology* (2011). doi:10.1586/ehm.11.30

150. Passaro, D., Quang, C. T. & Ghysdael, J. Calcineurin / CXCR4 in T-ALL. **2,** 781–782 (2015).